FILE COPY
NO 1

NACA TN 1350

NATIONAL ADVISORY COMMITTEE FOR AERONAUTICS

TECHNICAL NOTE

No. 1350

ESTIMATED LIFT-DRAG RATIOS AT SUPERSONIC SPEED

By Robert T. Jones

Ames Aeronautical Laboratory
Moffett Field, Calif.

REPRODUCED BY
NATIONAL TECHNICAL
INFORMATION SERVICE
U.S. DEPARTMENT OF COMMERCE
SPRINGFIELD, VA. 22161

Washington
July 1947

NATIONAL ADVISORY COMMITTEE FOR AERONAUTICS

TECHNICAL NOTE NO. 1350

ESTIMATED LIFT-DRAG RATIOS AT SUPERSONIC SPEED

By Robert T. Jones

SUMMARY

Recent developments in supersonic flow theory are applied to obtain estimates of the lift-drag ratios that may be achieved by aircraft employing swept-back wings. Lift-drag ratios greater than 10 to 1 can be maintained up to a Mach number of 1.4 by the use of large angles of sweep and high aspect ratios. As the speed increases in the supersonic range the attainable lift-drag ratios decrease and the gain due to sweepback also appears to diminish. An efficient configuration for M= 1.4 would require about 60° sweepback, an aspect ratio of 4 and a wing loading of one-third the atmospheric pressure. For a wing loading of 50 pounds per square foot the cruising altitude would be 60,000 feet and the indicated airspeed 290 miles per hour.

INTRODUCTION

The work required to propel an airplane a given distance in steady flight is equal to its weight times the distance travelled divided by the lift-drag ratio of the airplane. Hence the fuel expenditure per mile of flight need not increase with speed so long as the lift-drag ratio of the airplane can be maintained. However, with present shapes a prohibitive loss of lift-drag ratio occurs on passing beyond the speed of sound and it is evident that a radical change in configuration will be necessary for efficient flight at higher speeds.

The problem of an efficient configuration for flight at supersonic speeds was investigated by Busemann in 1935 (reference 1). Busemann concluded that an improvement in the lift-drag ratio at supersonic speeds could be obtained by sweeping the wing back at an angle just ahead of the Mach cone, but failed to recognize the relatively much greater

efficiencies obtainable when the wing is swept back behind the Mach cone. The change in the type of flow when the wing lies inside the Mach cone, and the resulting increase in efficiency have been brought out in reference 2. However, both reference 1 and reference 2 are restricted to considerations of two-dimensional flow and hence aspect-ratio effects could not be determined. Recent developments in aerodynamic theory have overcome this difficulty, making it possible to estimate the lift-drag ratio obtainable with practical configurations.

The present report applies these new theoretical results to obtain estimates of the lift-drag ratios that may be achieved with an efficient aircraft at supersonic speeds. The estimates are all based on the theory of small disturbances, first because this is the only adequate theory available, and second because it is reasoned that an aircraft producing a large disturbance in the external flow would be inherently inefficient.

At very high Mach numbers even thin bodies and small angles of attack cause relatively large pressure disturbances and consequent heating of the fluid. Here the heating effect of friction becomes no longer negligible. (Such conditions are likely to be encountered by rockets; however, in these cases the efficiency of steady flight may not be of primary concern.) The present analysis is therefore limited to more moderate speeds where the efficiency in steady flight is of primary importance and where it is evident that such efficiency can be achieved by known means.

FUNDAMENTAL RELATIONS FOR WING LOADING, ALTITUDE AND MAXIMUM LIFT-DRAG RATIO

The lift-drag ratio of a conventional airplane depends primarily on its external configuration and on the angle of attack and does not vary greatly with speed provided the correct relation between wing loading and altitude is maintained. For maximum efficiency the airplane should be flown at that lift coefficient $C_{L_{opt}}$ for which lift-drag ratio is a maximum. An increase in speed, then, necessitates an increase in altitude, since with fixed lift coefficient

(For a complete list of symbols see appendix.)

$$\frac{V}{V_o} = \sqrt{\frac{\rho_o}{\rho}} \tag{1}$$

where the subscript o refers to conditions at sea level.

With lift-drag ratio fixed, higher speed does not involve any increase in the thrust required for level flight; this thrust is simply

$$T = \frac{W}{(L/D)_{max}} \tag{2}$$

If the propulsive efficiency of the engine does not drop off with altitude, the increase in speed will thus be accomplished without any increase in the fuel consumption per mile of flight. Furthermore, the increase in speed is not accompanied by any significant change in the air loads or pressures on the airplane and hence no increase in structural stiffness is required. An obvious advantage of this method of increasing the cruising speed is that it does not interfere with the ability of the airplane to slow down at lower altitudes and land on short runways. A more complete discussion of these factors will be found in reference 3.

The altitude and speed of the airplane, of course, cannot be increased indefinitely at constant thrust, since eventually a critical Mach number will be exceeded and the lift-drag ratio of the airplane will begin to decrease. The limiting speed and the corresponding altitude may be determined from the relations

$$V = M_1 a \tag{3}$$

and

$$\frac{W/S}{\frac{\rho}{2}V^2} = C_{L_{opt}} \tag{4}$$

where M_1 is the Mach number at which, for $C_L = C_{L_{opt}}$, the drag begins to rise abruptly, a is the velocity of sound and W/S is the wing loading.

Equations (3) and (4) may be combined in the form

$$\frac{W/S}{p} = \frac{\gamma}{2} C_{L_{opt}} M_1^2 \tag{5}$$

where

p atmospheric pressure at altitude

γ ratio of specific heats for air (1.4).

Equation (5) gives the relation between wing loading and atmospheric pressure for maximum speed without loss of aerodynamic efficiency. This condition can hardly be attained at low altitudes since with an atmospheric pressure of 2000 pounds per square foot, for $M_1 = 0.75$ and the usual values of $C_{L_{opt}}$, the wing loading required would be of the order of 400 pounds per square foot. At 60,000 feet, however, the required wing loading works out to be the more practical value of 30 pounds per square foot.

Later calculations will show that similar considerations apply to supersonic aircraft; that is, the best lift-drag ratios are obtained when the wing loading is an appreciable fraction of the atmospheric pressure.

At subsonic speeds it is customary to divide the drag into two parts, one the result of friction (including the friction drag of the fuselage) and the other - the induced drag - the result of the lift. The friction drag is considered nearly independent of the angle of attack. Thus

$$C_D = C_{D_o} + C_{D_i} \tag{6}$$

where C_{D_o} is the drag at zero lift, and for subsonic flow equals C_{D_f}, the friction drag. If the velocity and pressure disturbances produced by the airplane are small, the drag arising from the lift will be satisfactorily represented by the well-known formula

$$C_{D_i} = \frac{C_L^2}{\pi A} \tag{7}$$

or

$$\frac{C_{D_i}}{C_L^2} = \frac{1}{\pi A} \tag{8}$$

and the friction drag will be nearly independent of the angle of attack. The lift-drag ratio at any angle is then

$$\frac{L}{D} = \frac{C_L}{C_{D_o}+C_{D_i}} \tag{9}$$

Solving for the lift coefficient at maximum lift-drag ratio results in

$$C_{L_{opt}} = \sqrt{\frac{C_{D_o}}{C_{D_i}/C_L^2}} \tag{10}$$

and therefore

$$\left(\frac{L}{D}\right)_{max} = \frac{1}{2}\sqrt{\frac{1}{C_{D_o}(C_{D_i}/C_L^2)}} \tag{11}$$

In calculating lift-drag ratio for supersonic speed the drag may again be divided into two components, one independent of the lift and one proportional to the square of the lift coefficient. However, in this case the drag at zero lift includes a pressure drag which varies with the thickness of the body or wing. Also, at supersonic speeds, the drag due to lift can no longer properly be called "induced drag." At subsonic speeds the drag arising from the lift can be traced to the influence of the trailing vortex wake on the wing - hence the designation "induced." At supersonic speeds, however, the forward influence of the wake usually constitutes only a small part of the drag arising from the lift and hence

the term "induced drag" does not seem appropriate. Different divisions of the drag due to lift into components of wave drag and induced drag have been proposed, but the proportions allotted in any particular case depend on the method of calculation employed. In the present report the drag is calculated by integrating the pressure distribution in the neighborhood of the body and in this case C_{D_i} appears simply as a pressure drag proportional to the square of the lift coefficient. The subscript i is retained to identify the law of variation with that of the induced drag at subsonic speeds.

Then, for comparison with the subsonic case, we may write

$$C_{D_o} = C_{D_f} + C_{D_t}$$

and

$$C_{D_i} = \left(\frac{C_{D_i}}{C_L^2}\right) C_L^2$$

where C_{D_f} is the total friction drag, and C_{D_t} the total thickness drag, due to wing and fuselage. The factor C_{D_i}/C_L^2 bears no simple relation to the aspect ratio as it does in the subsonic case, but is a complex function of the wing plan form and load distribution.

With the values of C_{D_o} and C_{D_i}/C_L^2, revised for supersonic conditions, equations (10) and (11) for the optimum lift coefficient and maximum value of the lift-drag ratio remain valid. Maximum L/D is obtained when the drag due to lift is equal to the drag at zero lift.

DRAG AT ZERO LIFT

Thickness Drag of Wings

The thickness drag of the wing may be calculated by the methods of reference 4 or 5. Figure 1 shows the variation of thickness drag with Mach number calculated by the method of reference 5 for a rectangular wing and for several swept-back wings. In these cases the airfoil is of symmetrical

biconvex section 5 percent thick. The results for the swept-back airfoils were obtained from reference 6. The curve for the rectangular airfoil is the same as that given for the infinite wing by the Ackeret theory since, as has been demonstrated by J. N. Nielsen in an unpublished application[1] of the same method, the integrated effect of removing outboard portions of the wing on the drag of the remainder of the wing is zero, at least so long as the Mach cone from each tip does not intersect the opposite tip. The thickness drag coefficient of the rectangular airfoil is therefore constant when

$$A\sqrt{M^2-1} > 1$$

where

A aspect ratio

When the wing is swept well behind the Mach cone the flow over most of the wing is of the subsonic type. (See reference 2.) The pressure drag is small and may be attributed to departures from the subsonic type of flow in the region of the root section. In this condition the outboard sections of the wing have little or no drag, and hence the drag coefficient is inversely proportional to the aspect ratio. At higher speeds, when the Mach angle approaches the leading-edge angle, the distribution of drag changes and the drag coefficient increases rapidly, particularly on the outboard sections. If the leading edge is too near the Mach cone, the drag of the swept wing will exceed that of the straight wing.

Figure 2 shows a plot similar to figure 1 of the variation of drag with Mach number for tapered swept-back airfoils. These results were obtained by K. Margolis of Langley Memorial Aeronautical Laboratory using the method of reference 5. An extensive series of calculations for tapered wings has been given recently by Stewart and Puckett (reference 7). In order to simplify the calculations a double-wedge section was assumed, though it is not to be

[1] Data on file at Ames Laboratory.

supposed that such a section would be desirable in practice. Here the angle of sweepback (60°) is that of the midchord line of the airfoils, which is also the line of maximum thickness. The sharp rises in drag coefficient near $M = 1.52$ and $M = 1.71$ occur when the Mach angle approaches the angle of the trailing edge. Evidently all generators of the wing surface must lie behind the Mach lines to insure favorable drag values.

According to the thin airfoil theory the calculated flow for a given airfoil plan form and Mach number will actually be similar to the flow over another plan form at a different Mach number, provided the two plan forms are oriented similarly with respect to the corresponding Mach lines. This relation may be preserved by changing the x coordinates of the plan form (fig. 3) in the proportion that the x coordinates of the Mach lines are changed, that is, as $\sqrt{M^2-1}$. For plan forms having similar flow patterns the ratio

$$m = \frac{\text{cot leading-edge angle}}{\text{cot sweep angle of Mach lines}}$$ will be constant.

The aspect ratio will then vary with Mach number according to

$$A\sqrt{M^2-1} = \text{constant} \tag{12}$$

and thin airfoil theory shows that the drag coefficient will be proportional to

$$\frac{(t/c)^2}{\sqrt{M^2-1}}$$

or

$$C_{D_t}\sqrt{M^2-1} \sim (t/c)^2 \tag{13}$$

where t/c is the thickness-chord ratio measured in the stream direction. Figure 4 shows the coefficient

$$\frac{C_{D_t}\sqrt{M^2-1}}{(t/c)^2}$$

plotted against m for the constant-chord biconvex airfoils.

Friction Drag of Wing

In general, the friction drag of the wing will be of the same order of magnitude as the thickness drag. At very high speeds a considerable amount of heat is generated in the boundary layer and the resultant temperature variation affects the magnitude of the skin friction. For moderate supersonic speeds, however, the heating effect is not large and the normal relation of skin friction to Reynolds number will not be greatly modified.

For present purposes a conservative value of $C_{D_f} = 0.006$ corresponding to a turbulent boundary layer at a Reynolds number of 10^7 has been used.

Drag of Fuselage

A method for calculating the wave drag of a slender fuselage at supersonic speeds was given by von Kármán in 1935 (reference 8). This method was applied in reference 9 to a series of bodies of parabolic arc shape and estimates of the friction drag added to obtain total drag. More recently the calculations of Haack (reference 10), Sears (reference 11), and Lighthill (reference 12) have become available. These investigators apply Karman's method to the determination of body forms having a minimum wave drag for certain conditions. The minimum problem is solved for three cases: viz, I, given volume and given length; II, given length and given diameter; and III, given diameter and given volume.

The following equations may be obtained[2] from Haack's report (reference 10). The length l is so chosen that the body lies between +1 and -1 on the x-axis; r/r_o is the radius at any station in terms of the maximum radius r_o and a is the frontal area πr_o^2. The volume is given in terms of the volume of the circumscribed cylinder, and the drag coefficient, which does not include friction, is given in

[2]The formulas given as the final relations in the report are in error. However, the correct relations can easily be derived from the preceding equations.

terms of the frontal area. The factor d/l is the fineness ratio, diameter/length.

Case I: Given length, given volume

$$\left.\begin{aligned} \left(\frac{r}{r_o}\right)^2 &= \left(\sqrt{1-x^2}\right)^3 \\ \text{Volume} &= \frac{3}{16}\,\pi l\,\pi r_o^2 \\ C_D &= \frac{9}{8}\,\pi^2\left(\frac{d}{l}\right)^2 \end{aligned}\right\} \quad (14)$$

Case II: Given length, given diameter

$$\left.\begin{aligned} \left(\frac{r}{r_o}\right)^2 &= \sqrt{1-x^2} - x^2\cosh^{-1}\frac{1}{x} \\ \text{Volume} &= \frac{\pi}{6}\,l\,\pi r_o^2 \\ C_D &= \pi^2\left(\frac{d}{l}\right)^2 \end{aligned}\right\} \quad (15)$$

Case III: Given diameter, given volume

$$\left.\begin{aligned} \left(\frac{r}{r_o}\right)^2 &= 3\sqrt{1-x^2} - 2\left(\sqrt{1-x^2}\right)^3 - 3x^2\cosh^{-1}\frac{1}{x} \\ \text{Volume} &= \frac{\pi}{8}\,l\,\pi r_o^2 \\ C_D &= \frac{3}{2}\,\pi^2\left(\frac{d}{l}\right)^2 \end{aligned}\right\} \quad (16)$$

Figure 5 shows the body shapes computed from these formulas.

Although the wave drag diminishes with increasing slenderness, the friction drag for a given volume or a given cross section tends to increase because of the greater surface area. With usual values of the friction coefficient a favorable balance between the two components requires such a slender body that in most cases the dimensions will actually be governed by the minimum allowable cross section. For a slender body the surface area and hence the friction drag associated with a given cross section is proportional to l/d, while the wave drag is proportional to $(d/l)^2$. It follows that the total drag will be a minimum when the slenderness ratio is such that the friction drag is twice the wave drag.

It will be noted that the body shape for case I actually has very little more drag than the case II body of the same diameter, and since body I has a greater useful volume, it seems a logical choice for practical design. Figure 6 shows the wave drag for case I and also the total drag, based on a skin-friction coefficient of 0.0021, as a function of the fineness ratio. The value of this friction coefficient was obtained from reference 13, and corresponds to a fully turbulent boundary layer and a Reynolds number of 10^8. With this friction coefficient the optimum fineness ratio is about 16 to 1.

DRAG DUE TO LIFT

The drag due to lift is estimated from theoretical solutions for the supersonic flow over thin lifting surfaces. Theoretical solutions are known for cases in which the lifting surface is curved and twisted in such a way as to support a uniform load (reference 14) and, for certain rectangular, triangular, or tapered flat surfaces (references 14 and 15).

Uniformly Loaded Surface

The solution for the uniformly loaded surface may be derived by methods similar to those described in reference 5 for the nonlifting airfoil. In that report the pressure due to thickness on an airfoil oblique to the stream was obtained by superposing the effects of oblique line sources in the acceleration potential field. The effect of a line source is

to cause a deflection of the stream lines crossing the source like the deflection caused by a thin wedge-shaped body; that is, the line source is followed by an area over which the vertical velocity w is constant and of opposite sign above and below the chord plane.

Similarly, an oblique vortex gives rise to a constant difference in the horizontal velocity increment u, and therefore in the pressure, above and below the plane of flow crossing the vortex. The corresponding w for a semi-infinite vortex is given by

$$w = \frac{u}{\pi m}\left(\sqrt{1-m^2}\cosh^{-1}\frac{x'}{|y'|} - \cosh^{-1}\frac{x}{|y|}\right) \tag{17}$$

where $x' = x - my$ and y' denotes the absolute value of $y - mx$ (The geometry of the figure has been adjusted, as described in the preceding section and reference 5, to correspond to the case in which the Mach angle is 45°; that is, $\sqrt{M^2-1} = 1$.)

The shape of the surface and the constant pressure are related to the velocity increments by the following formulas:

$$\frac{dz}{dx} = \frac{w}{V} \tag{18}$$

and

$$\frac{\Delta p}{q} = \frac{2u}{V} \tag{19}$$

Thus the camber of a triangular airfoil shaped to support a uniform load (fig. 7) may be obtained by superimposing two oblique vortices to form a V coinciding with the leading edge of the triangle. Integration of equation (17) for this case yields:

$$z = \frac{C_L}{4\pi m}\left[\frac{\sqrt{1-m^2}}{m}\left(\bar{y}'\cosh^{-1}\frac{\bar{x}'}{|\bar{y}'|} - y'\cosh^{-1}\frac{x'}{|y'|}\right)\right.$$
$$\left. -2\left(x\cosh^{-1}\frac{x}{|y|} - \sqrt{x^2-y^2}\right)\right] \qquad (20)$$

where

$$\bar{x}' = x + my \text{ and } \bar{y}' = y + mx$$

To obtain a lifting surface of finite chord it is necessary to introduce a negative V-shaped vortex at the desired chord length downstream. (See fig. 8.) Through the use of a finite number of straight vortex segments any plan form bounded by straight lines can be obtained.

The variation of w over the area enclosed by the vortex segments not only gives the camber and twist of the surface required to support a uniform load, but also can be used to calculate the drag arising from the lift. It can be seen that, since the pressure distribution is uniform over the section, the resultant force will lie in a direction at right angles to the chord line, or the line joining the leading and trailing edge, regardless of the camber of the surface. Hence the angle of attack of the chord line at any section times the lift gives the drag due to lift at that section.

In case the leading edge of the airfoil is ahead of the Mach cone the uniformly loaded surface is flat over portions of the wing not influenced by the root or the tip, as is given by the Ackeret theory. More interesting cases are those in which the leading edges are swept behind the Mach cone.

In the case of the swept-back wing it is found that the angle of attack has a logarithmic infinity at the center section. Hence the wing would require an infinite twist to maintain the uniform load across this section. At a distance from the center section the shape of the lifting surface resembles that of the familiar "constant load mean line" used

for subsonic airfoils. The twist and hence the section drag disappear rapidly with distance from the center section. There is consequently a marked reduction of drag coefficient with increasing aspect ratio, just as in the case of the drag due to thickness.

The infinite twist required at the root section, of course, makes the construction of such a wing impractical. We may conclude that in a practical wing there will be some falling off of the lift across the center section, and calculations of the lift distribution for flat surfaces show such a loss. The uniformly loaded airfoil gives a useful picture of the variation of drag with plan form, however. In spite of the fact that the local drag coefficient at the root section tends toward infinity, the integrated or over-all drag coefficient of the swept-back wing is finite and at reasonable aspect ratios is considerably lower than that of the flat unswept wing.

Figure 9 shows the coefficient of drag due to lift C_{D_i}/C_L for a series of uniformly loaded airfoils having a constant chord and varying degrees of sweep. To simplify the calculations, an approximation was made for the effect of the wing tip. With the tip cut off parallel to the direction of flight a large twist would theoretically have been required to maintain the uniform load right out to the tip. Instead of calculating this additional twist at the tip, the shape of the infinite wing with uniform load was assumed without modification and a loss in lift within the Mach cone originating at each tip was taken into account. Since the lift will have the full value along the boundary of the cone and will fall to zero at the tip, an average value of half the full load was used over this region. Since the effect of this approximation to a tip effect on the total drag value was small, any error involved in the approximation must also be small. If the tip were cut off along the Mach lines, slightly lower values of C_{D_i}/C_L would have been obtained.

Figure 9 shows that the values of C_{D_i}/C_L at supersonic speed are in general higher than the value corresponding to the same aspect ratio at subsonic speed but approach this value as the angle of sweep is increased (i.e., as $m \to 0$). The practical difficulty of maintaining a given aspect ratio of course increases as the angle of sweep is increased.

Flat Lifting Surfaces

Rectangular plan form.- For a flat rectangular wing of infinite aspect ratio the Ackeret theory gives

$$\frac{\partial C_L}{\partial \alpha} = \frac{4}{\sqrt{M^2-1}} \tag{21}$$

Since the lift is at right angles to the chord,

$$C_{D_i} = C_L \times \alpha \tag{22}$$

and

$$\frac{1}{\sqrt{M^2-1}} \frac{C_{D_i}}{C_L^2} = 0.25 \tag{23}$$

At a Mach number of 1.4 this value is nearly five times the drag due to lift of a subsonic airfoil of aspect ratio 6.

If the wing has a finite aspect ratio there will be a reduction of lift at the tip and a consequent reduction in $\partial C_L/\partial \alpha$ from the value given by equation (21). The distribution of lift over the tip of a flat rectangular wing has been calculated by Busemann (reference 14). The lift over the portion of the wing between the tip Mach cones (fig. 10) is constant and equal to that given by the Ackeret theory. Within either tip cone the lift pressure falls from this value to zero at the tip. If y/x represents the fractional distance from the tip toward the Mach line at a given chordwise position, then the lift pressure varies according to the function

$$\frac{4\alpha}{\sqrt{M^2-1}} \cos^{-1}\left(1 - 2\frac{y}{x}\right) \tag{24}$$

Superposing the effects of the two tip cones where they overlap and integrating the pressure over the whole wing gives for the lift coefficient

$$C_L = \frac{4\alpha}{\sqrt{M^2-1}} \frac{A\sqrt{M^2-1} - \frac{1}{2}}{A\sqrt{M^2-1}} \tag{25}$$

and for the drag due to lift

$$\frac{1}{\sqrt{M^2-1}} \left(\frac{C_{D_i}}{C_L{}^2}\right) = \frac{A\sqrt{M^2-1}}{4A\sqrt{M^2-1} - 2} \tag{26}$$

Busemann's solution is valid for $A\sqrt{M^2-1} \geq 1.0$, that is, so long as the Mach cone from one tip does not cross over the opposite tip. It is interesting to note that when $A\sqrt{M^2-1}=1.0$ the lift falls to zero along the whole trailing edge and the span load distribution is elliptical, as shown in reference 16 for airfoils of very low aspect ratio.

Triangular plan form.- Formulas for the lift distribution and $\partial C_L/\partial\alpha$ for a flat triangular airfoil behind the Mach cone have been given recently by Stewart (reference 15). Stewart finds that the lift distribution as predicted from elementary considerations for very slender triangles (reference 16) actually holds for all leading-edge angles until the leading edge touches the Mach cone. Stewart finds also

$$\sqrt{M^2-1}\,\frac{\partial C_L}{\partial\alpha} = \frac{2\pi m}{E} \tag{27}$$

where $E = E(\sqrt{1-m^2})$ is the elliptic integral.

In the case of the flat surface with the leading edge behind the Mach cone, the chordwise lift distribution has an

infinite value at the leading edge just as it does in the subsonic case. Here the resultant force will be inclined forward relative to the chord plane because of the suction force at the leading edge.

The drag due to lift for the flat triangular airfoil was evaluated by setting up the complex expression for the velocity field u and w by means of Busemann's method (reference 14). The drag was then calculated from the formula

$$C_D = \int_c \frac{2u}{V} \times \frac{w}{V} \, ds \tag{28}$$

by integrating around a contour c a short distance away from the airfoil surface and enclosing the singularity at the leading edge. The result is

$$\frac{1}{\sqrt{M^2-1}} \frac{C_{D_i}}{C_L{}^2} = \frac{2E - \sqrt{1 - m^2}}{4\pi m} \tag{29}$$

A similar formula has been given recently by W. D. Hayes (reference 17).

In this formula, the first term represents a drag equal to the lift times the angle of attack, and the second term represents the thrust at the leading edge. It is noted that this latter term disappears progressively as the edge approaches the Mach cone (i.e., $A\sqrt{M^2-1} \to 4$). At the other limit, the slender triangle near the center of the Mach cone, $E \to 1$, and

$$\frac{C_{D_i}}{C_L{}^2} = \frac{1}{\pi A} \tag{30}$$

as in reference 16. Although the theory shows a forward thrust on the thin plate with a sharp edge, it is not to be expected that this characteristic will be realized in practice unless the leading edge is given a finite radius or camber.

Tapered plan form.- The theoretical lift distribution for a flat untapered swept-back wing with the leading edge behind the Mach cone has not yet been determined. However, the solution for the flat triangular wing may be readily extended to include a special family of tapered wings. This extension is based on the fact that an area of the triangular wing may be removed by making cuts along Mach lines without affecting the flow over the area remaining ahead of the cuts. In particular, the removal of such area will not affect the suction force on the leading edge, as long as the area removed does not include any of the leading edge so that the coefficient of thrust will be increased as area is cut away. Evidently the most efficient members of this family of airfoils are those in which the maximum area is cut out of the triangle, that is, the wing is tapered to a point. (See fig. 11).

With the trailing edge fixed at the Mach angle, the angle of taper and hence the aspect ratio of these wings varies with the angle of sweep in such a manner that

$$\sqrt{M^2-1}\,A = \frac{4m}{1-m} \tag{31}$$

as the leading edge approaches the Mach cone $m \to 1.0$ and the aspect ratio approaches infinity.

The lift-curve slope of these airfoils is determined simply by integrating the pressure distribution for the triangular airfoil over the appropriate area. The calculation gives

$$\sqrt{M^2-1}\,\frac{\partial C_L}{\partial \alpha} = \frac{4m}{\sqrt{1-m^2}}\,\frac{1}{E}\left(\frac{\cos^{-1}(-m)}{1+m} + m\sqrt{\frac{1-m}{1+m}}\right) \tag{32}$$

and for the drag due to lift

$$\frac{1}{\sqrt{M^2-1}}\frac{C_{D_i}}{C_L{}^2} = \frac{1}{\sqrt{M^2-1}\,\frac{\partial C_L}{\partial \alpha}} - \sqrt{\frac{1+m}{1-m}}\,\frac{1}{4m}\,N^2 \tag{33}$$

where N is the ratio of the lift-curve slope of the triangular airfoil to that of the tapered airfoil, that is,

$$N = \frac{(\pi/2)\sqrt{1-m^2}}{\frac{\cos^{-1}(-m)}{1+m} + m\sqrt{\frac{1-m}{1+m}}} \tag{34}$$

Equations (31) through (34) apply to the case of the wing tapered to a point. In subsonic flow such extreme taper is known to lead to high local lift coefficients over the tip portions and to the possibility of tip stalling even at moderate lift coefficients. A similar tendency is evident at supersonic speeds; in fact, the section lift coefficients tend toward infinity at the pointed tip. Hence the extreme taper should not be used in practice and value of $C_{D_i}/C_L{}^2$ calculated for these cases will be somewhat optimistic.

Comparison of Lift and Drag Values for Flat Surfaces

Curves showing the variation of lift-curve slope with Mach number and aspect ratio for the rectangular, triangular, and tapered airfoils are shown in figure 12. At $A\sqrt{M^2-1} = 4$ the leading edge of the triangular airfoil touches the Mach cone and, as shown by Puckett (reference 4), the lift characteristics at higher aspect ratios are identical with those of a rectangular airfoil of infinite aspect ratio.

The drag due to lift versus aspect ratio for the various flat wings is shown in figure 13. According to the Ackeret theory

$$\frac{1}{\sqrt{M^2-1}}\frac{C_{D_i}}{C_L{}^2} = \frac{1}{4} \tag{35}$$

and it is to be noted that both the rectangular and the

triangular airfoils approach this value at higher aspect ratios. At

$$A\sqrt{M^2-1}<4 \qquad (36)$$

the leading edges of the triangular airfoil are behind the Mach cone and the drag due to lift is reduced somewhat because of the suction on the leading edge. However, the really favorable values of $C_{D_i}/C_L{}^2$ are obtained only with the swept-back wings of relatively high aspect ratio. The fact that the values for the flat pointed wings agree with those for the cambered, untapered airfoils shown on figure 9 is an indication that the drag due to lift is primarily a function of sweepback and aspect ratio.

RESULTS

The total drag of the supersonic aircraft can now be estimated by adding up the components thus far considered with an allowance for the friction drag of the wing and a small allowance for the tail surfaces.

Since the lift-drag ratio increases with increasing slenderness of the wing, it is necessary to establish some standard of slenderness to obtain comparative values. A rough measure of the structural stiffness of a wing is the maximum spar depth at the wing root divided by the distance, measured along the spar, to the centroid of area of the wing. A value of 1/15 seems to be about the limit of present-day construction.

Airplane with Constant Chord Swept-back Wing

Figure 14 shows lift-drag ratios obtainable at $M = 1.4$ as a function of m with a configuration embodying the constant chord, uniform lift airfoil and a type I body of 15 to 1 fineness ratio. An allowance of $C_{D_f} = 0.006$ was made for the friction drag on the wing and a value equal to 10 percent of the wing drag was allotted to the vertical tail. No horizontal tail is shown, since it is not clear that such a tail would be required with this configuration. The frontal area of the body was assumed to be 4 percent of the wing area. The drag and lift of the wing were assumed to carry across the center sections.

without being modified by the presence of the body.

The airfoil shape is obtained by superimposing a parabolic arc thickness distribution upon a cambered and twisted surface designed, as discussed earlier, to support a uniform load. The varion in sweepback, or m, in this case was assumed to be obtained by rotating the wing panels without changing their length-width ratio, hence the aspect ratio varies with sweep as shown. The wing in the unswept position would have an aspect ratio of 12. If the ratio of the root thickness to the spar length from the root section to the centroid of the wing panel is 1/15, the thickness-chord ratio of the unswept wing would be 0.2. The same wing rotated through 60° (m = 0.577) has an aspect ratio of 3 and a t/c (c measured parallel to the stream) of 0.1.

The calculations for the uniformly loaded wings show higher lift-drag ratios for still higher aspect ratios and greater thickness-chord ratios, but it is doubtful that the calculations based on the theory of small disturbances apply in these cases.

Because of the higher aspect ratios attainable with a tapered wing it is found that these configurations are more efficient than the constant chord wings, and therefore they will be discussed in somewhat greater detail.

Airplane with Tapered Wing

Figure 15 shows the lift-drag ratios obtainable at M = 1.4 with the flat pointed wing. The proportions of fuselage and tail are the same as in the preceding case, and the same value of C_{D_f} was used. The calculations were made assuming double-wedge sections (as in fig. 2), but an approximate correction factor of 4/3 was inserted into the thickness drag to take account of the greater average slope of the biconvex profile. The quantity 4/3 is the ratio of the wave drag of the biconvex section to that of the double-wedge section in two-dimensional flow. The maximum wing thickness in each case is again 1/15 the distance from the wing root to the centroid of area of the half wing. The variation of t/c (streamwise) is shown in figure 15. Since the trailing-edge angle is fixed on the Mach line, the aspect ratio increases indefinitely as m approaches 1, according to equation (31). The optimum lift coefficient

calculated by equation (10), is also shown in figure 15.

Figure 16 shows the variation of $(L/D)_{max}$ with m at different Mach numbers. It is noted that the optimum value of m is different for different Mach numbers; there appears to be no fixed relation between the sweepback angle and the Mach angle. Evidently relatively greater sweepback angles should be used at smaller Mach numbers. The optimum values of m will, of course, be influenced by the magnitude of the friction drag.

DISCUSSION OF RESULTS

Effect of Plan Form

Figure 17 shows the lift-drag ratios replotted against aspect ratio and compared with values estimated for a straight wing-body combination. It will be noted that up to M = 2 the swept-back wing is much more efficient than the straight wing. The difference is smaller at the higher Mach numbers, however, and the advantages of sweepback at very high Mach numbers may be questioned. In each case the efficiency diminishes with Mach number.

Although the configurations shown in figures 14 and 15 appear from the calculations to give the best lift-drag ratios, it is not to be assumed that these configurations are actually the most suitable for practical use. In practice the wing must of course have a finite tip chord and may also require some camber or twist to avoid the high concentration of load near the tips. Also, as has been previously remarked, the location of the trailing edge on, rather than behind, the Mach lines was chiefly a computational device. It is probable that a greater sweep of the trailing edge would be desirable.

Such modifications will of course cause changes in the lift-drag ratio. However, it is believed that the highest lift-drag values shown can actually be approached with practical configurations. The theoretical values of C_{D_i}/C_L^2 for the wing with its trailing edge along the Mach cone are somewhat more favorable than the values to be expected with a wing having its trailing edge behind the Mach cone. On the other hand, the location of the trailing edge along the Mach line is unfavorable from the standpoint of thickness drag, as shown by figure 2. Hence the net effect of trailing-edge location on

$(L/D)_{max}$ is not expected to be very pronounced. The beneficial effects of tapering the wing indicated by figure 17 may also be assumed to hold qualitatively for more moderate degrees of taper.

Airfoil Section

No attempt was made in the analysis to find an optimum airfoil profile. The section assumed for the calculations has a parabolic thickness distribution. In practice, as previously mentioned, it would be necessary to round or camber the leading edge to achieve the predicted values of C_{D_i}/C_L^2. It might also be advantageous to use (with the tapered plan form) a cusped trailing edge. This device would enable the designer to take advantage of the high lift to be obtained by placing the trailing edge along the Mach lines, while effectively giving the thickness distribution a greater angle of sweep and thus averting the large wave drag which arises when the generators of the thickness distribution are too near the Mach lines.

Friction Drag

The allowance of 0.006 made for the friction drag coefficient of the wing corresponds to a turbulent boundary layer at a Reynolds number of 10^7. The assumption of turbulent friction for both wing and fuselage is believed to be conservative, since there are indications that large areas of laminar flow can be achieved at supersonic speeds. The importance of maintaining laminar flow or otherwise reducing the friction can be seen from the magnitudes of the various drag components with the best configuration (fig. 15, m = 0.5) at a Mach number of 1.4. The various components are shown in the following table:

(1)	Thickness drag of wing	0.0041
(2)	Friction drag of wing	.0060
(3)	Thickness drag of body	.0020
(4)	Friction drag of body	.0036
(5)	Drag of vertical tail	.0010
Total drag at zero lift:	C_{D_o} =	.0167
Drag due to lift	C_{D_i} =	.0167
Total drag		0.0334
Friction drag (2) + (4)		0.0096

Note that the friction drag is more than 50 percent of the total drag at zero lift. In this case the maximum lift-drag ratio is 10.7; with completely laminar flow the ratio would increase to about 15.

Optimum Wing Loading and Altitude

The analysis indicates that reasonably good aerodynamic efficiencies are obtainable up to Mach numbers of 1.5. At $M = 1.4$ the best configuration studied should operate near a lift coefficient of 0.35. From equation (5), the wing loading for this case works out to be about one-half the atmospheric pressure. This pressure disturbance can no longer be considered small and the question arises as to whether the linearized theory can be considered applicable in this case. No accurate analysis of this limitation can be given at present. However, an approximate criterion can be deduced by comparing the flow over the swept-back wing with the two-dimensional subsonic flow over a wing section at the same component Mach number as suggested in reference 2. When this comparison is made for configurations near the optimum in figure 15 it is found that the wing sections are operating beyond their critical Mach numbers at the indicated optimum lift coefficient. Thus it appears that the optimum lift coefficient will actually be smaller than is indicated by the linearized theory. For the best configuration at $M = 1.4$, it appears that the optimum lift coefficient may be nearer 0.25 than the 0.357 indicated by figure 15. In this case the L/D_{max} will be diminished from 10.7 to 10, and the optimum wing loading from one-half to approximately one-third atmospheric pressure. At sea level the wing loading required would be 700 pounds per square foot, but for operation at 60,000 feet the much more reasonable figure of 50 pounds per square foot is obtained. At this altitude the true airspeed is 900 miles per hour and the indicated airspeed 290 miles per hour.

Ames Aeronautical Laboratory,
National Advisory Committee for Aeronautics,
Moffett Field, Calif., May 1947.

APPENDIX

SYMBOLS

V	flight velocity
V_o	velocity at sea level
ρ	air density
ρ_o	density at sea level
p	atmospheric pressure
T	thrust
W	weight
L	lift
D	drag
M	Mach number $\left(\frac{V}{a}\right)$
a	velocity of sound
C_L	lift coefficient $\left(\frac{L}{\rho/2\ V^2S}\right)$
S	wing area
γ	ratio of specific heats ($\gamma = 1.4$ for air)
C_D	drag coefficient $\left(\frac{D}{\rho/2\ V^2S}\right)$
C_{D_o}	drag coefficient at zero lift
C_{D_t}	coefficient of drag due to thickness
C_{D_i}	coefficient of drag due to lift
C_{D_f}	friction drag coefficient

A	aspect ratio
b	wing span (perpendicular to direction of flight)
x	coordinate along direction of flight
m	parameter indicating relative slope of wing leading edge $\left(m = \frac{\text{cotangent leading-edge angle}}{\text{cotangent sweep angle of Mach lines}} \right)$
t	thickness of wing at midchord
c	wing chord
l	length of fuselage
r	radius of fuselage
r_o	maximum radius
d	maximum diameter of fuselage $(d = 2r_o)$
w	small vertical velocity disturbance
u	small horizontal velocity disturbance
y	lateral (spanwise) coordinate
x'	$x - my$ $\overline{x}' = x + my$
y'	$y - mx$ $\overline{y}' = y + mx$
z	vertical coordinate of wing camber line
α	angle of attack
E	complete elliptic integral of the second kind
N	ratio of lift-curve slope of triangular airfoil to that of the tapered airfoil

REFERENCES

1. Busemann, A.: Aerodynamischer Auftrieb bei Uberschallgeschwindigkeit. Luftfahrtforschung, Bd. 12, Nr. 6, Oct. 3, 1935.

2. Jones, Robert T.: Wing Plan Forms for High-Speed Flight. NACA TN No. 1033, 1946.

3. Korvin-Kroukovsky, B. V.: High Altitude Aviation. Aviation Magazine, April 20, 1929 and May 18, 1929.

4. Puckett, Allen E.: Supersonic Wave Drag of Thin Airfoils. Jour. Aero. Sci., vol. 13, no. 9, Sept. 1946, pp. 475-484.

5. Jones, Robert T.: Thin Oblique Airfoils at Supersonic Speed. NACA TN No. 1107, 1946.

6. Harmon, Sidney M. and Swanson, Margaret D.: Calculations of the Supersonic Wave Drag of Nonlifting Wings with Arbitrary Sweepback and Aspect Ratio Wings Swept Behind the Mach Lines. NACA TN No. 1319, 1947.

7. Stewart, H. J. and Puckett, A.E.: Aerodynamic Performance of Delta Wings at Supersonic Speeds. Paper presented at the 15th Annual Meeting of the Institute of the Aeronautical Sciences New York, January 1947.

8. von Kármán, Th.: The Problem of Resistance in Compressible Fluids. GALCIT Pub. No. 75, 1936. (From R. Accad. d'Italia, cl. Sci. fis., mat. e nat., vol. XIV, 1936.)

9. Jones, Robert T. and Margolic, Kenneth.: Flow Over a Slender Body of Revolution at Supersonic Velocities. NACA TN No. 1081, 1946.

10. Haack, W.: Geschossformen kleinsten Wellenwiderstandes. Bericht 139 der Lilienthal Gesselschaft.

11. Sears, William R.: On the Minimum Wave Drag of Projectiles. Quarterly of Applied Mathematics. Jan. 1947, pp. 361-366.

12. Lighthill, M. J.: Supersonic Flow past Bodies of Revolution. R. & M. No. 2003, British A.R.C., 1945.

13. Young, A. D.: The Calculation of the Total and Skin Friction Drags of Bodies of Revolution at Zero Incidence. R. & M. No. 1874, British A.R.C., 1939.

14. Busemann, A.: Infinitesimale kegelige Uberschallstromung. Sonderdruck. Jahrbuch 1942/43 der Deutschen Akademie der Luftfahrtforschung.

15. Stewart, H. J.: Lift of a Delta Wing at Supersonic Speeds. Quarterly Appl. Math., vol. IV, no. 3, Oct. 1946, pp. 246-254.

16. Jones, Robert T.: Properties of Low-Aspect Ratio Pointed Wings at Speeds below and above the Speed of Sound. NACA TN No. 1032, 1946.

17. Hayes, W. D.: Linearized Theory of Conical Supersonic Flow with Application to Triangular Wings. North American Aviation Co., Engineering Dept. report No. NA-46-818, Oct., 1946.

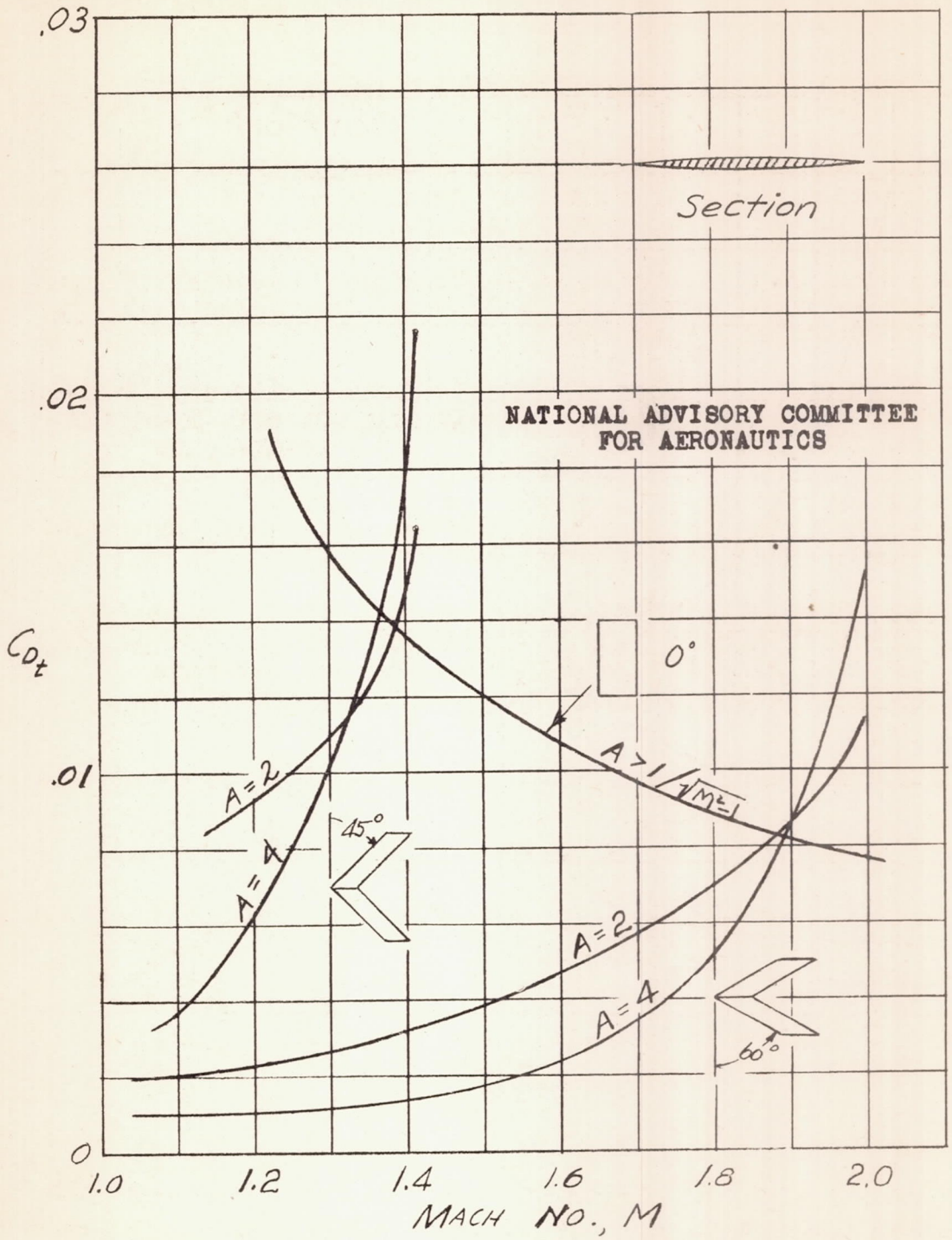


Figure 1. – Thickness drag coefficient for straight and swept-back wings; biconvex section, 5 percent thick.

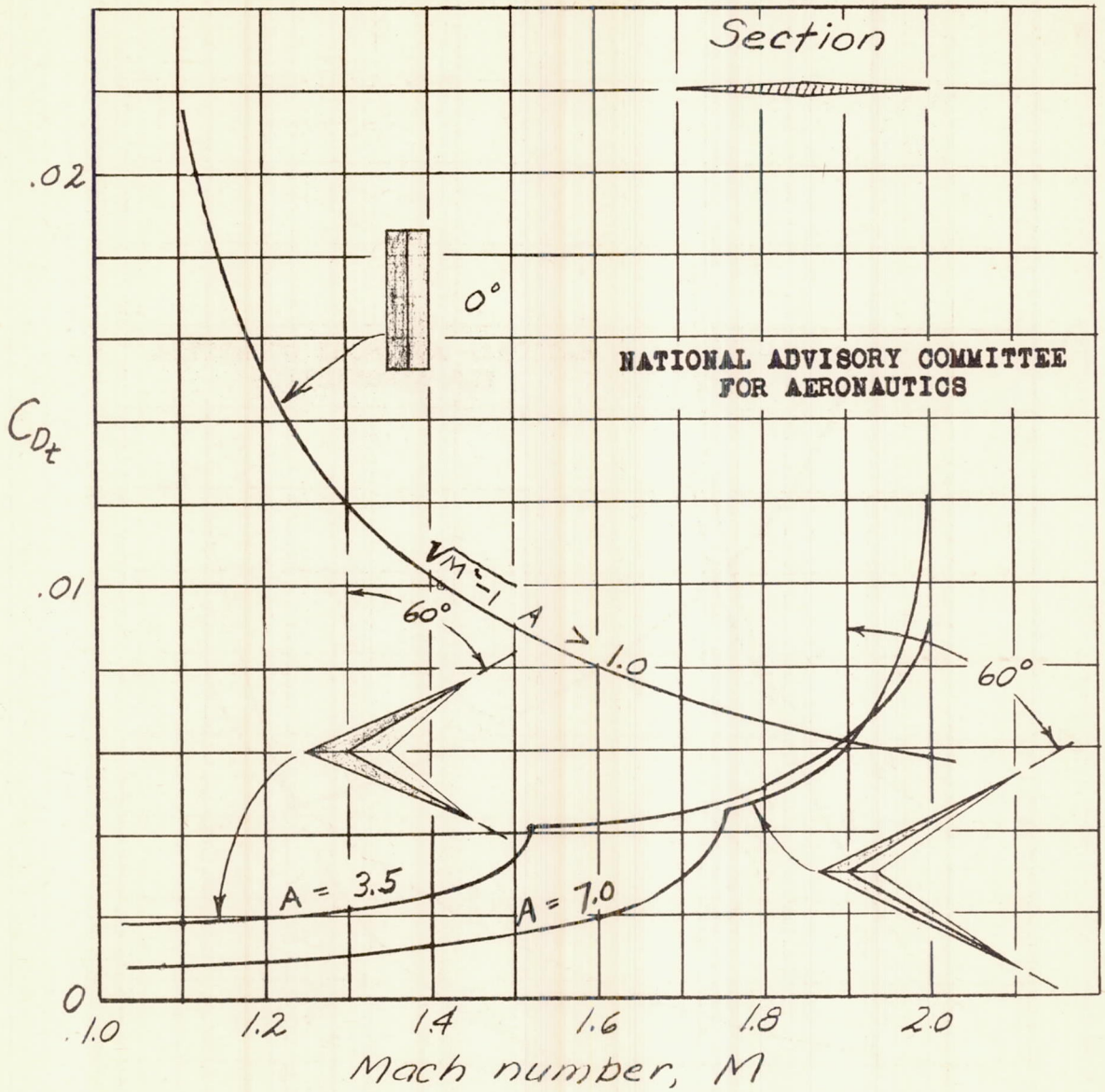
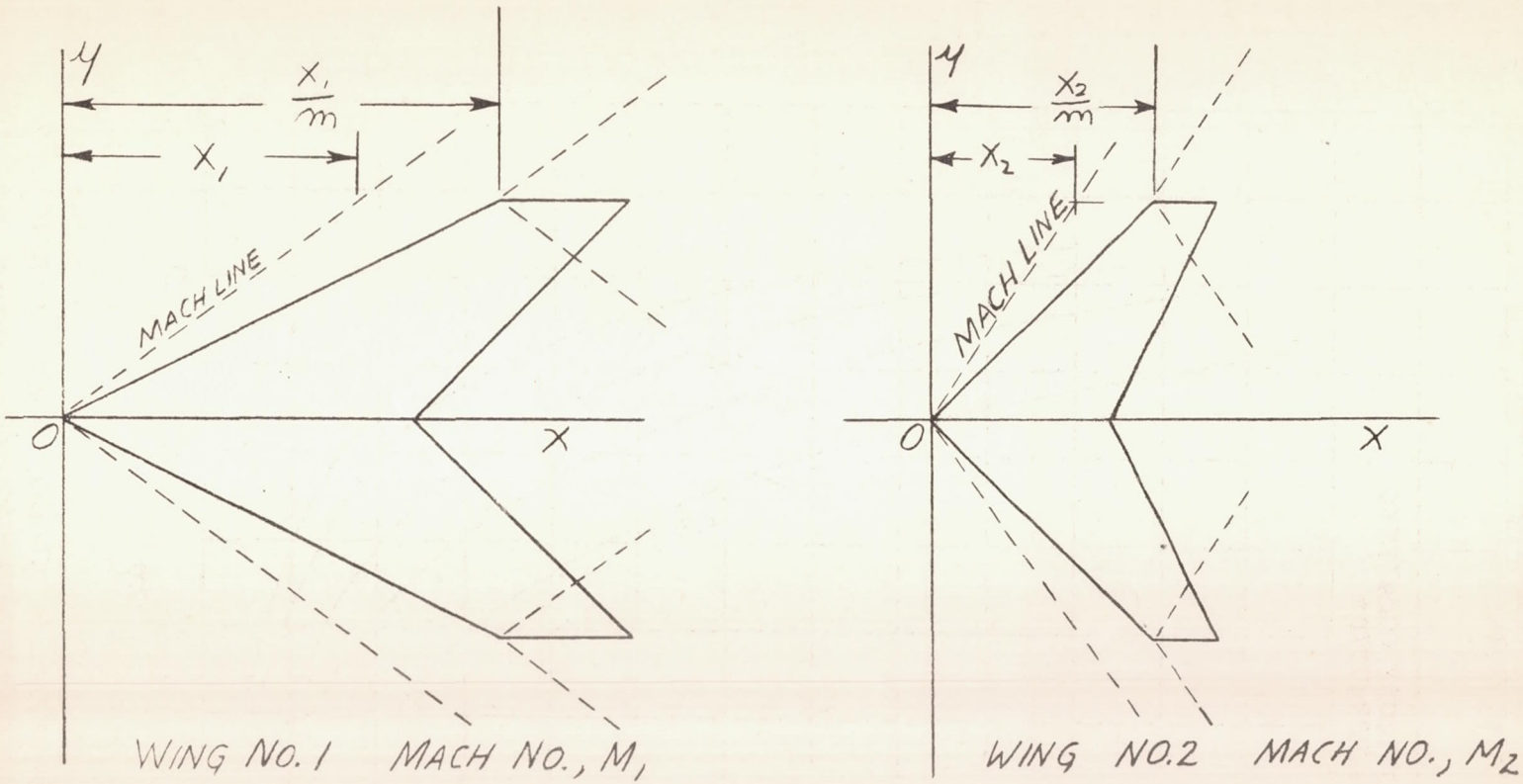


Figure 2.- Thickness drag coefficients for tapered swept-back wings compared with straight wing. Double-wedge sections, 5 percent thick.



NATIONAL ADVISORY COMMITTEE
FOR AERONAUTICS

$$\alpha_1 = \alpha_2 \; ; \left(\frac{t}{c}\right)_1 = \left(\frac{t}{c}\right)_2 \; ; \left(\frac{\Delta p}{q}\right)_1 = \left(\frac{\Delta p}{q}\right)_2 \frac{x_2}{x_1}$$

FIGURE 3. — WINGS HAVING SIMILAR FLOW PATTERNS AT DIFFERENT MACH NUMBERS.

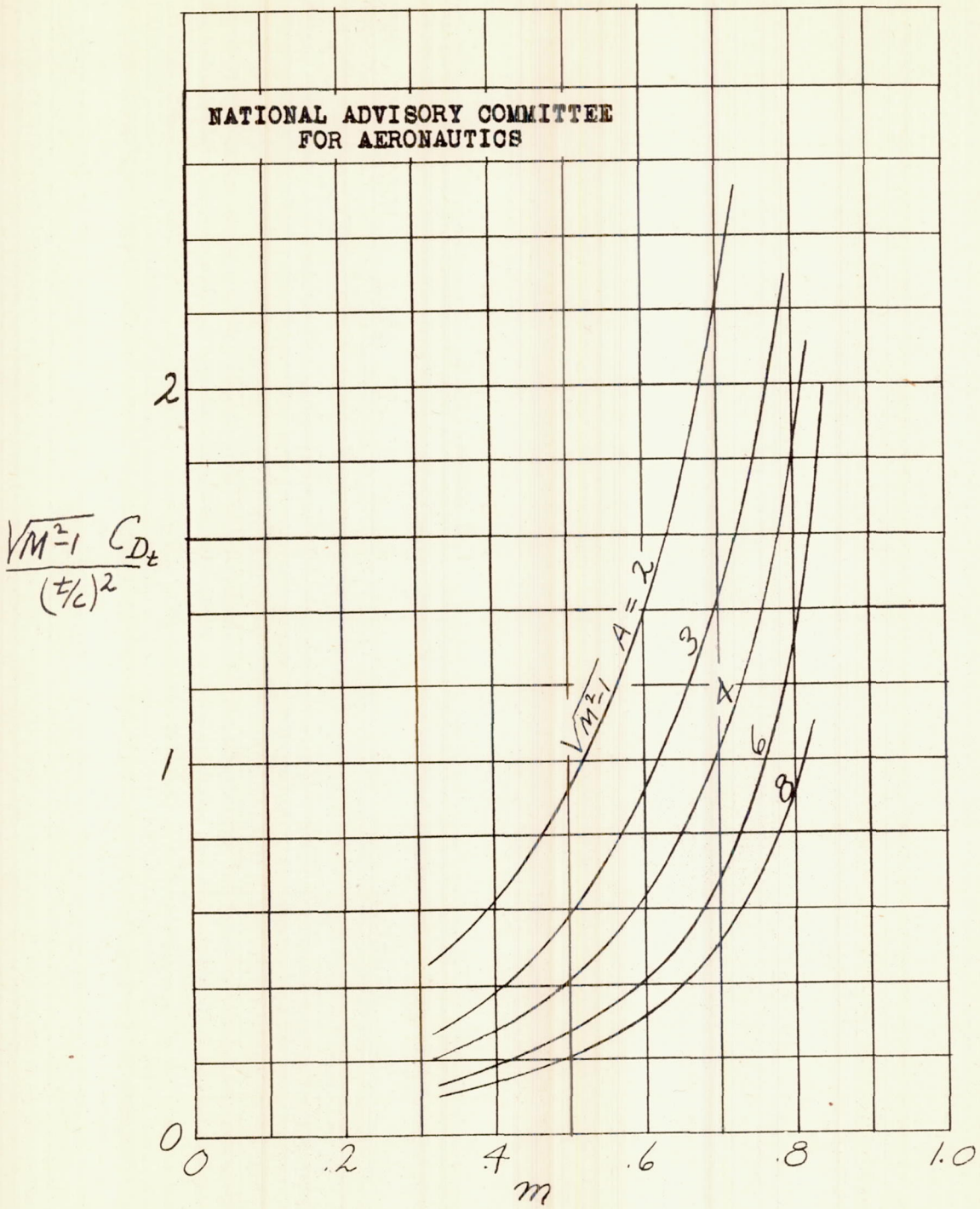


Figure 4 - Thickness drag coefficient for constant-chord sweptback wings of biconvex section.

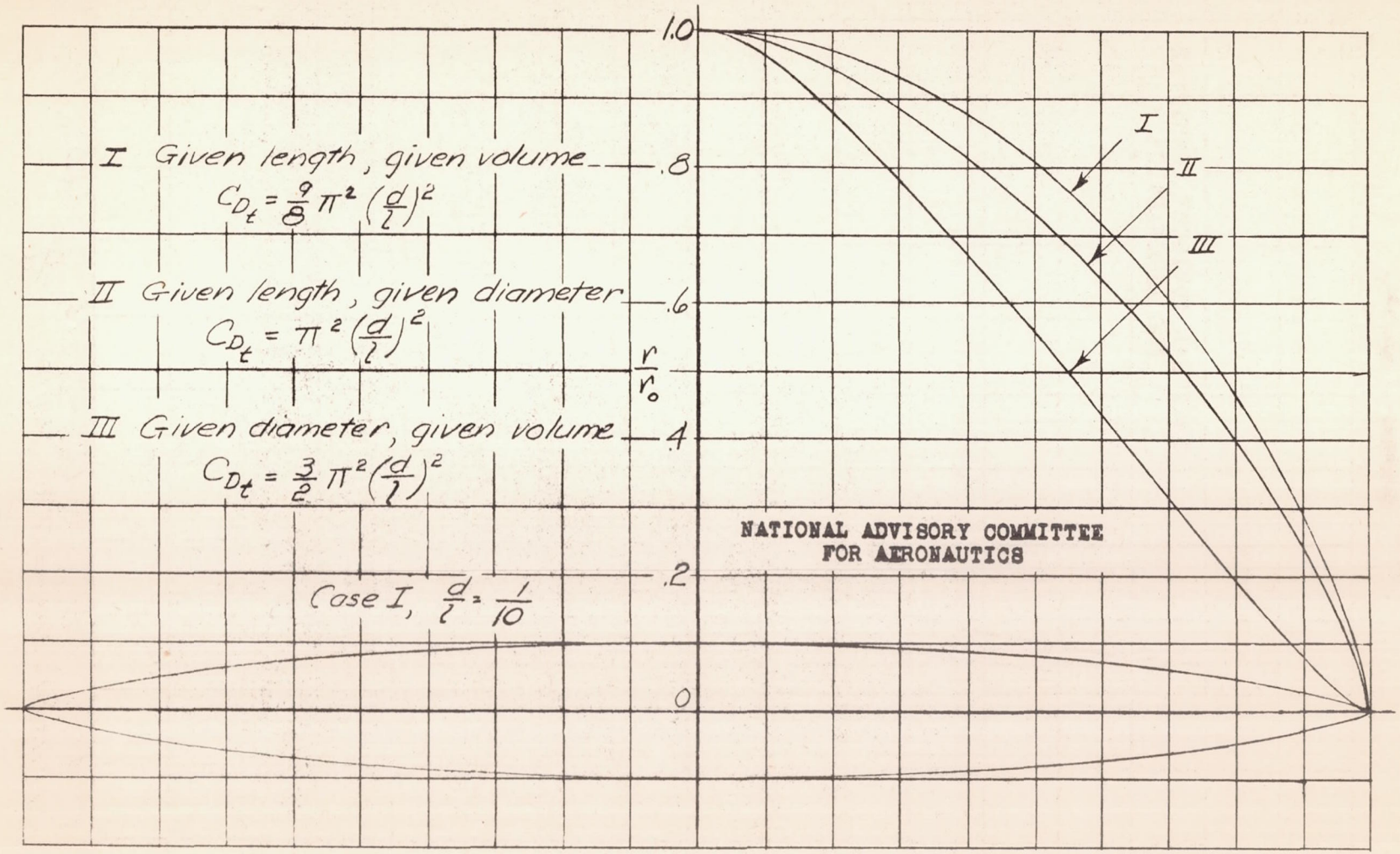


Figure 5.— Bodies of revolution having the minimum wave drag for different specifications of length, diameter and volume. (Ref. 10).

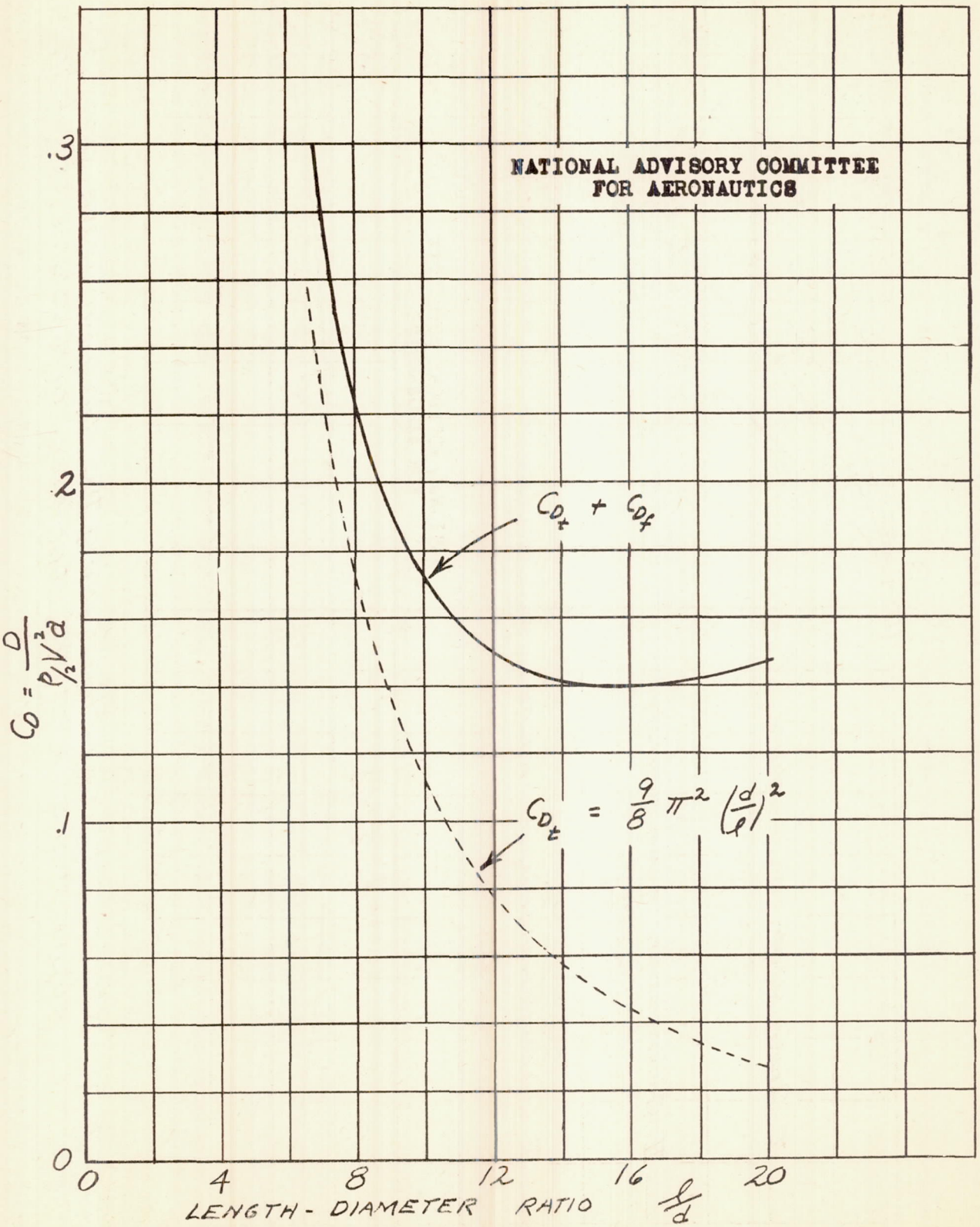


FIGURE 6 — DRAG COEFFICIENT OF FUSELAGE I

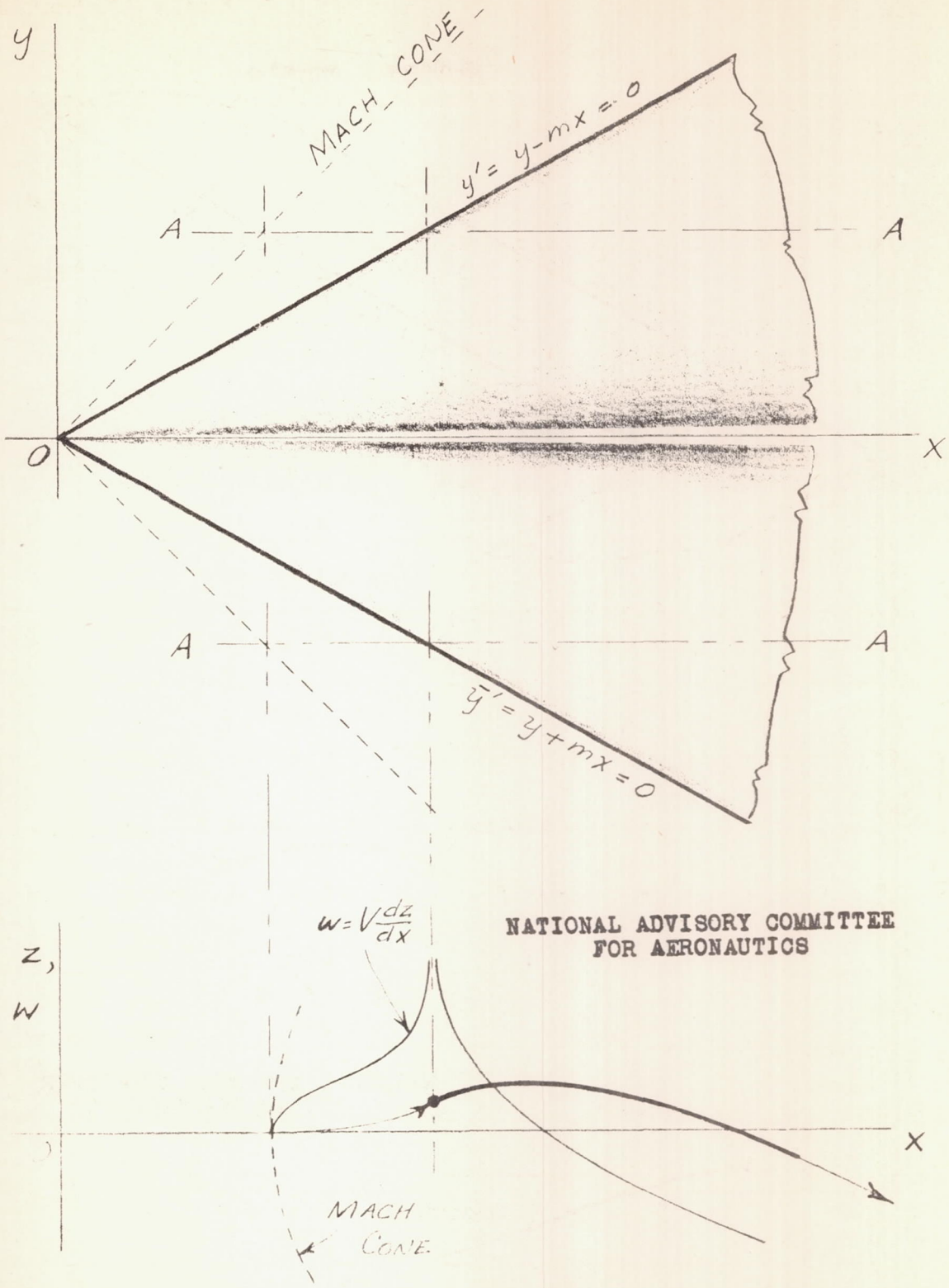
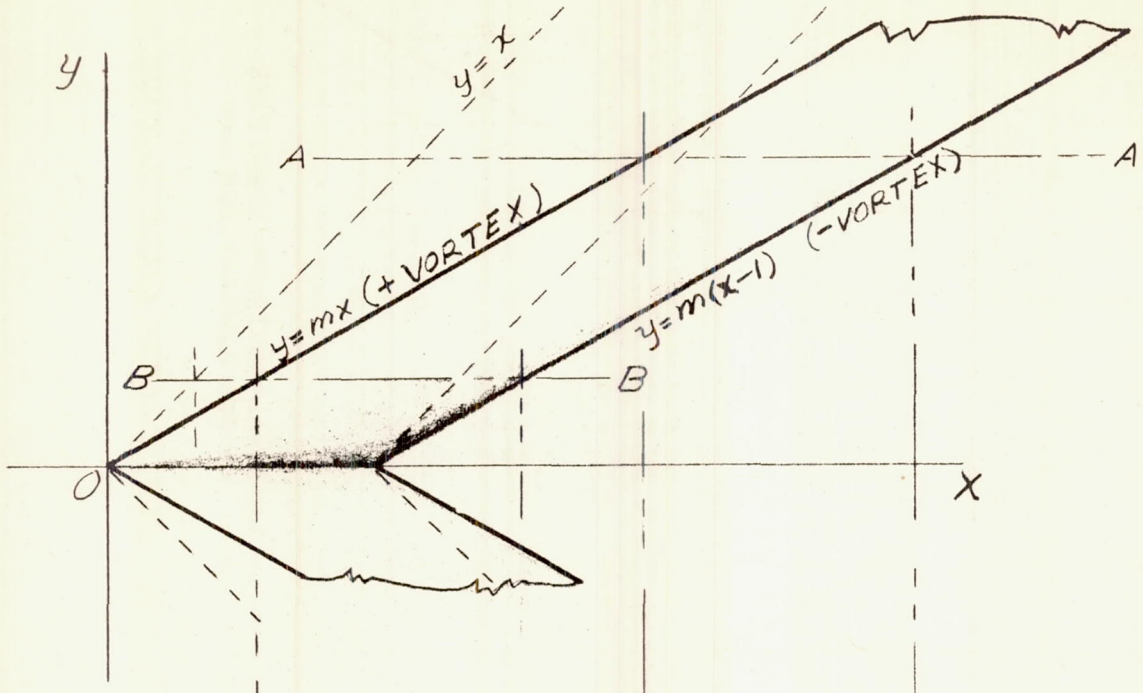
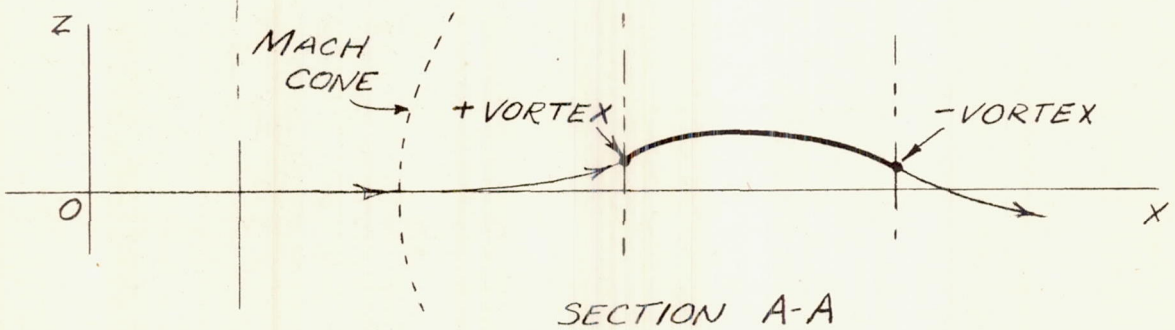
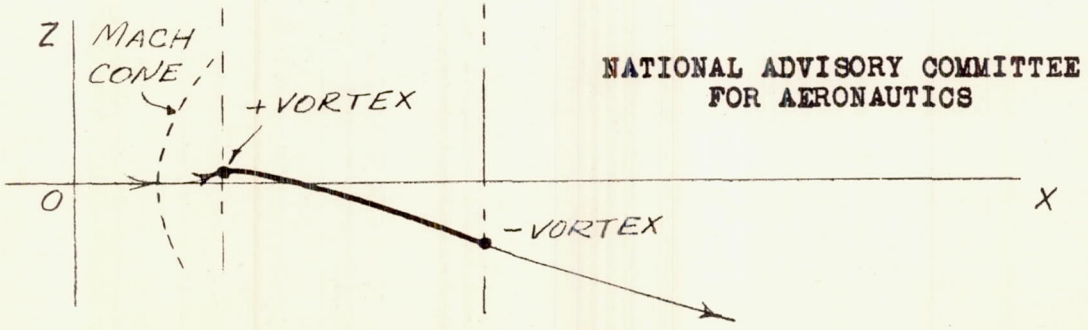


FIGURE 7.- UNIFORMLY LOADED TRIANGLE FORMED BY V-SHAPED VORTEX.





SECTION A-A



SECTION B-B

NATIONAL ADVISORY COMMITTEE FOR AERONAUTICS

FIGURE 8.- STREAMLINES AND CAMBER SHAPES FOR UNIFORMLY LOADED SURFACE.

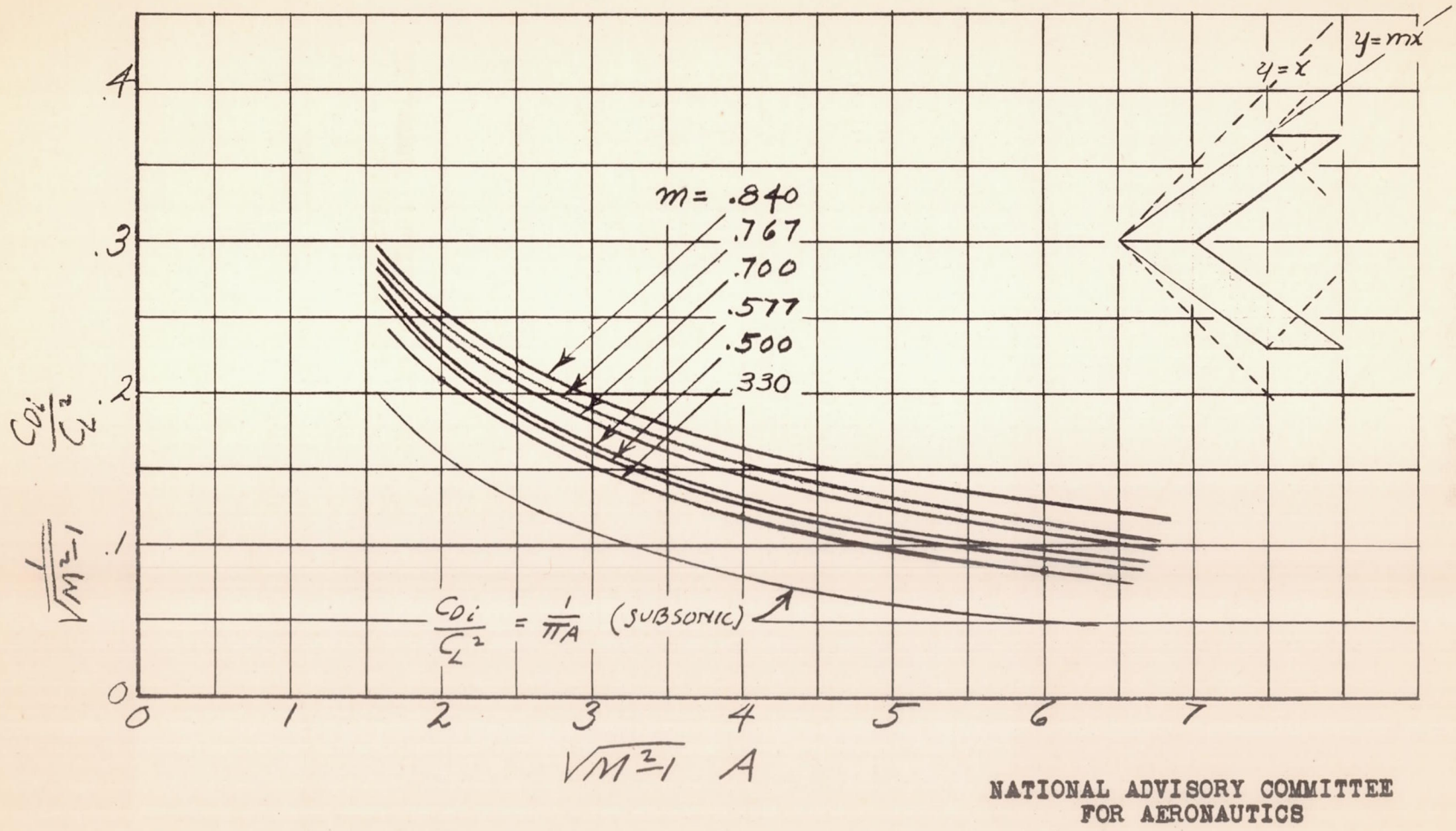


Figure 9. — Coefficient of drag due to lift for swept-back wings with uniform distribution of load.

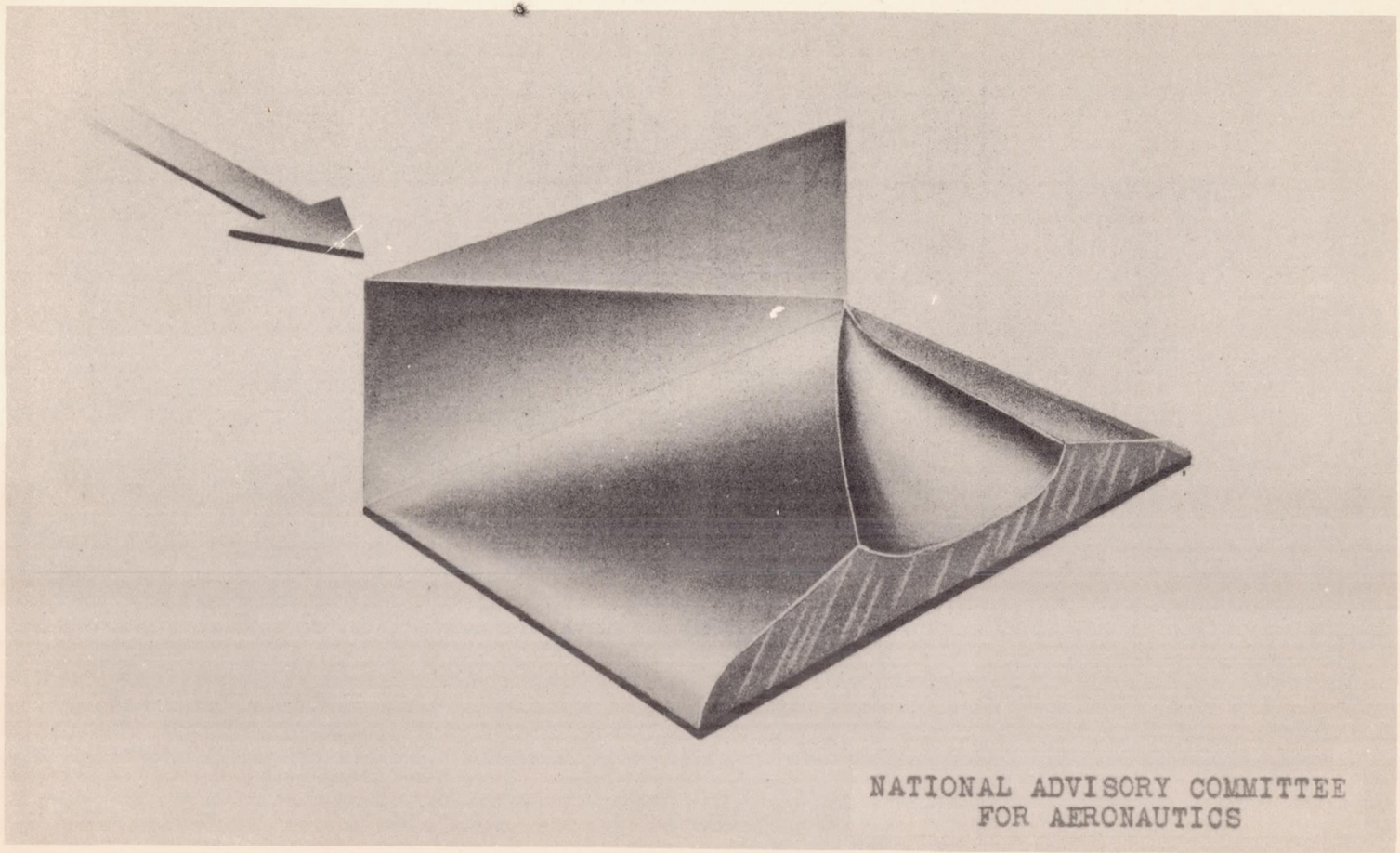


Figure 10.- Lift distribution over flat rectangular surface (ref. 7).

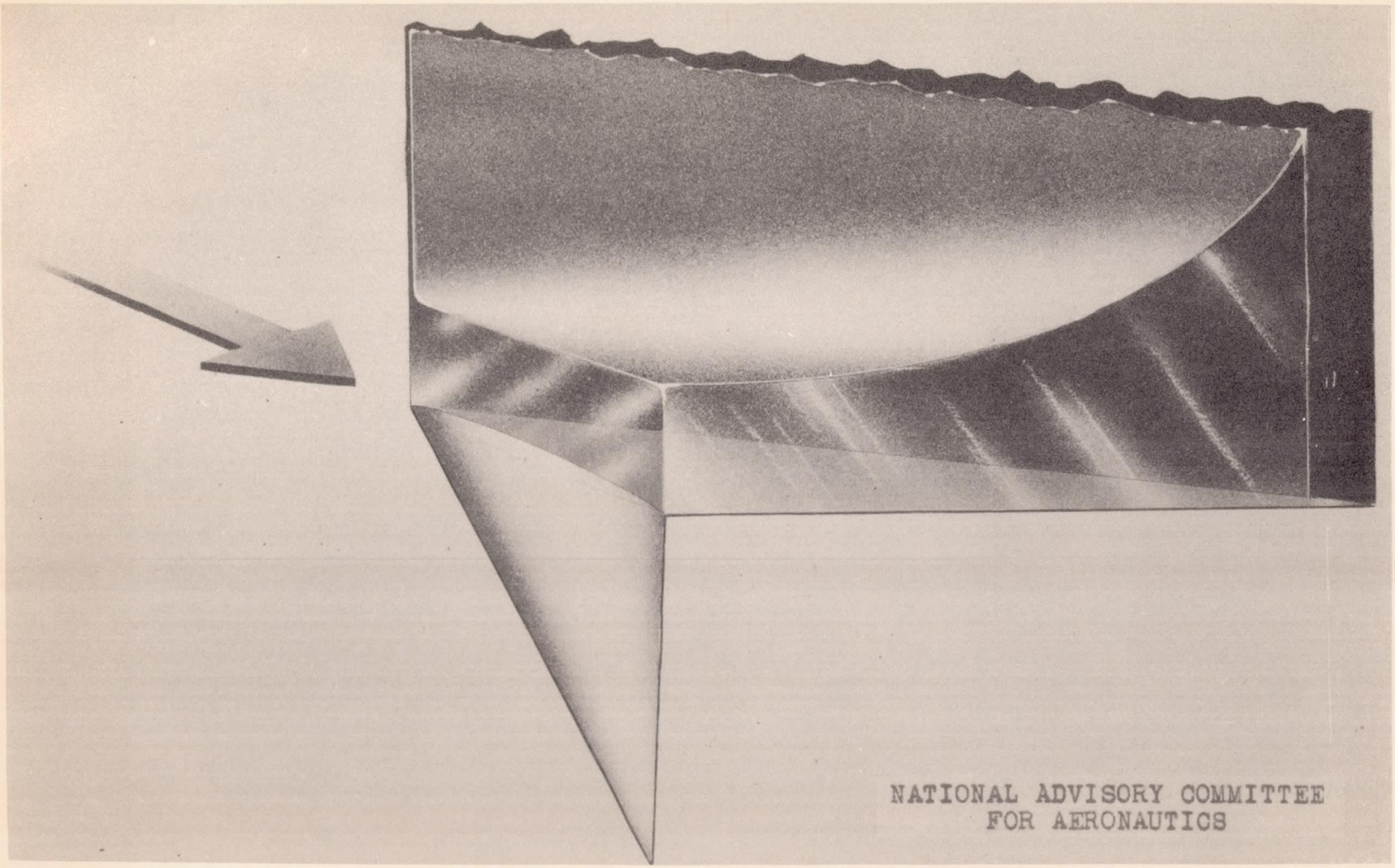


Figure 11.- Lift distribution over swept-back tapered wing with trailing edges along Mach lines.

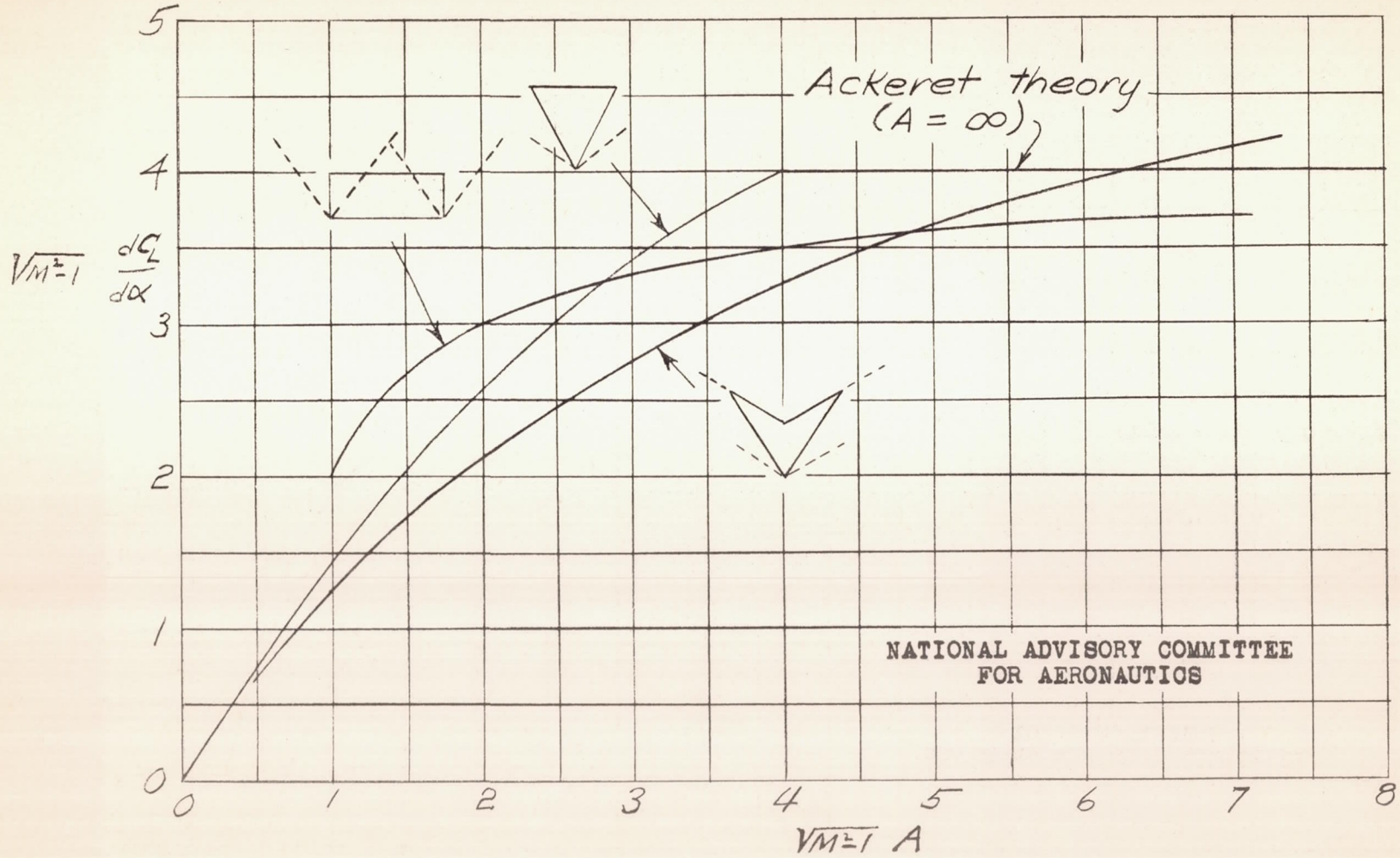


Figure 12. – Lift-curve slope as a function of aspect ratio

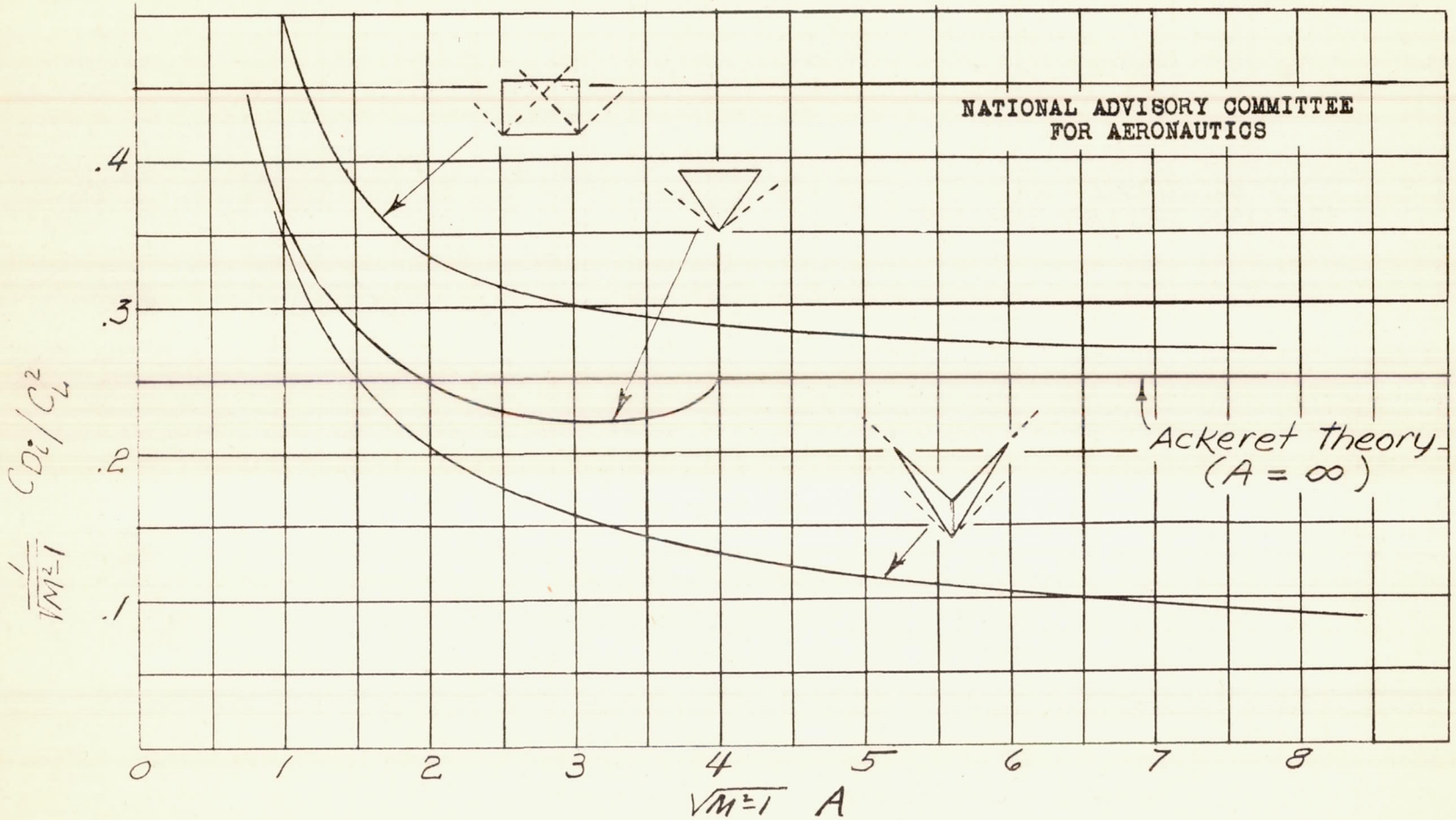


Figure 13 - Drag due to lift as a function of aspect ratio, flat wings

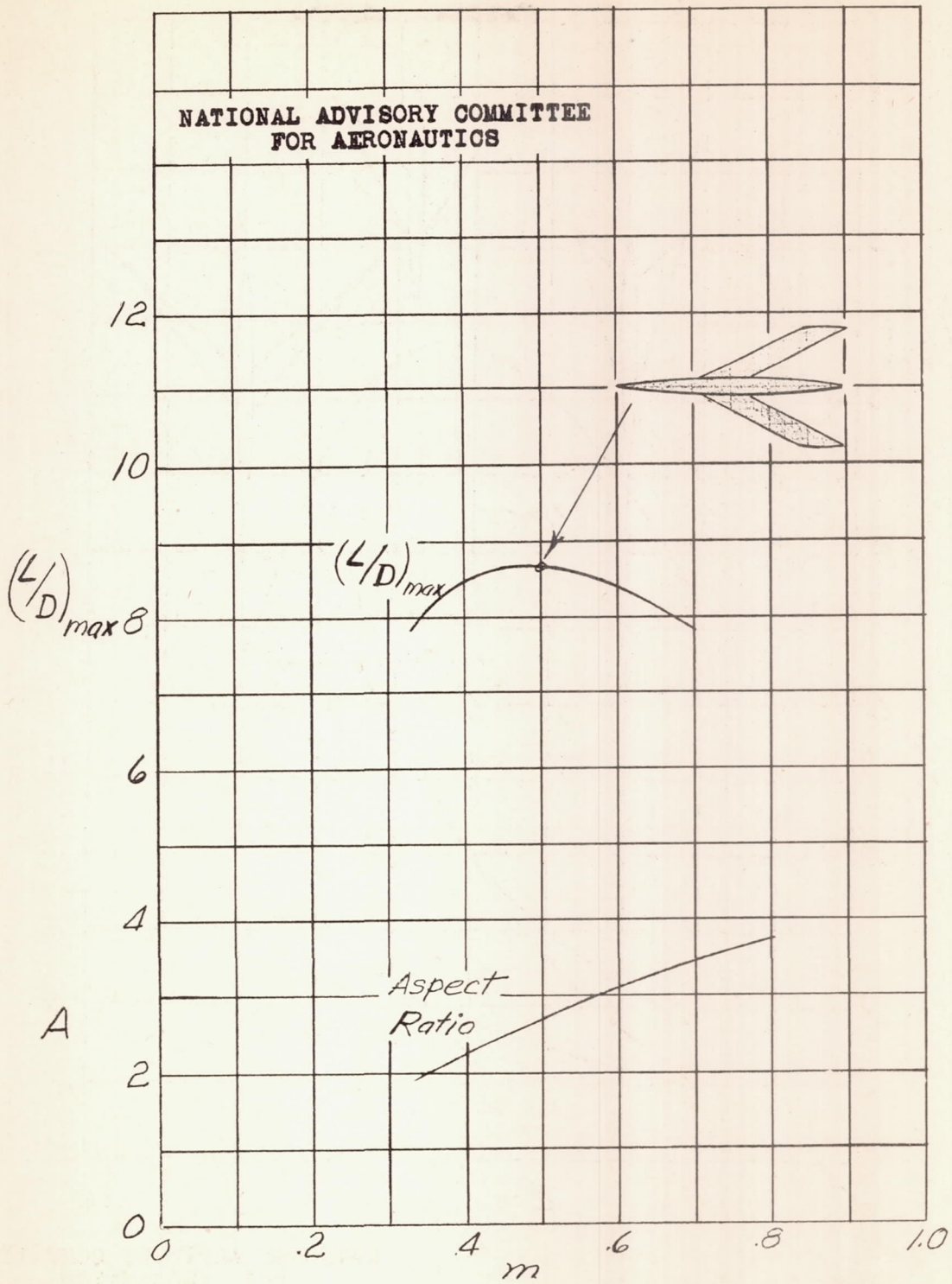


Figure 14 - $(L/D)_{max}$ for airplane with uniformly loaded, constant-chord wings; M = 1.4.

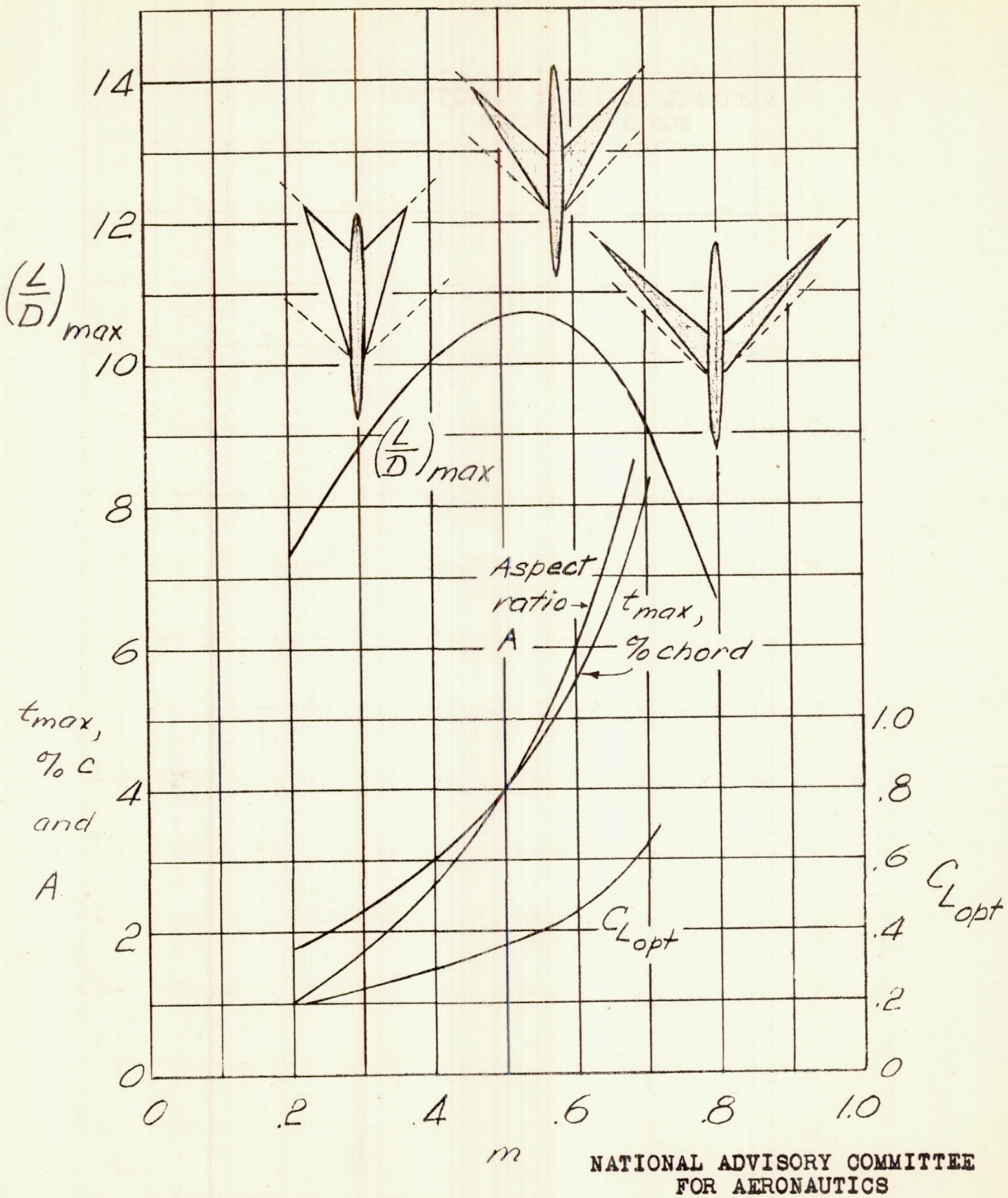


Figure 15. — $(L/D)_{max}$ and $C_{L_{opt}}$ for tapered wing configurations with varying sweep. M=1.4.

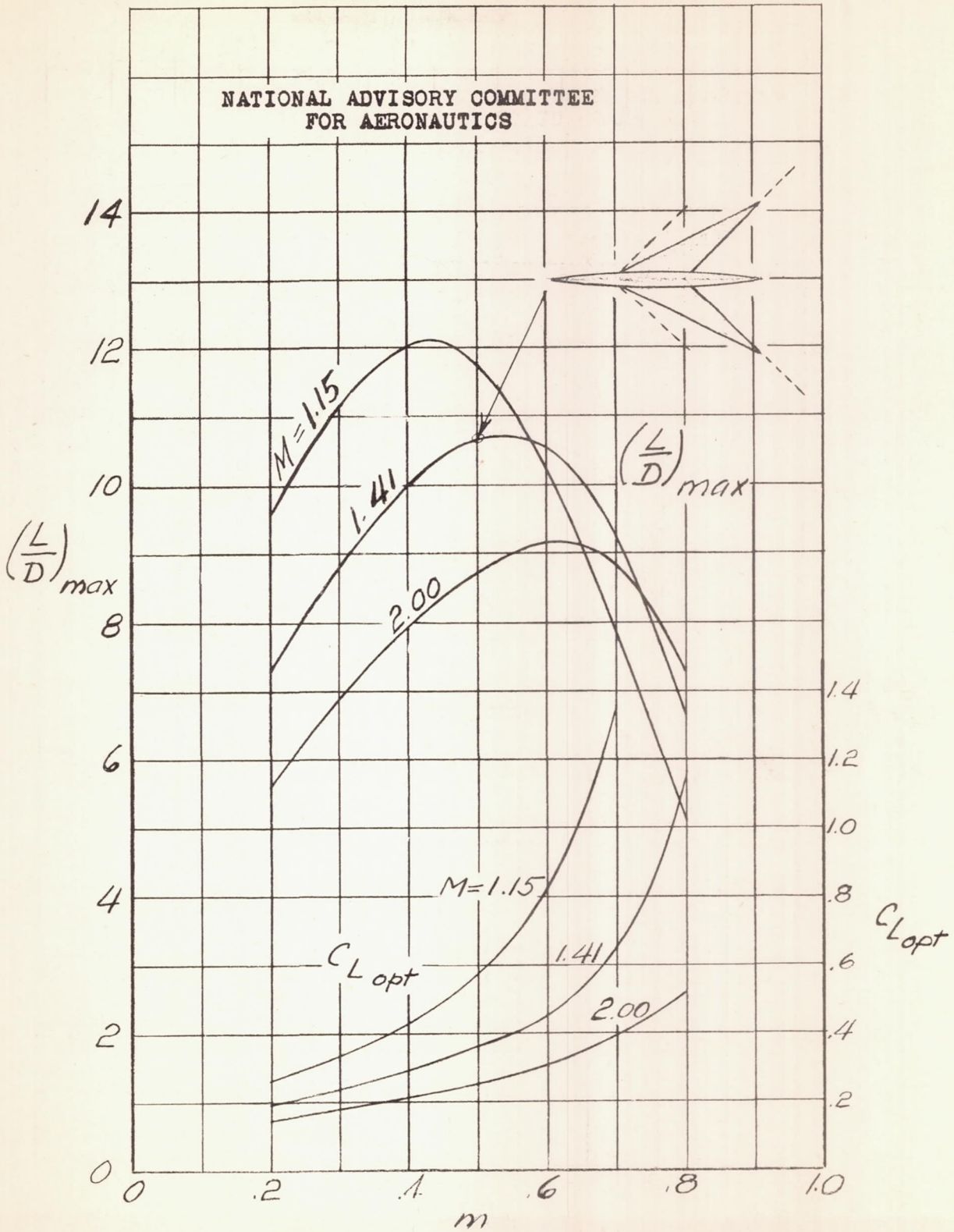


Figure 16.- $(L/D)_{max}$ for airplanes with tapered sweptback wings at various Mach numbers.

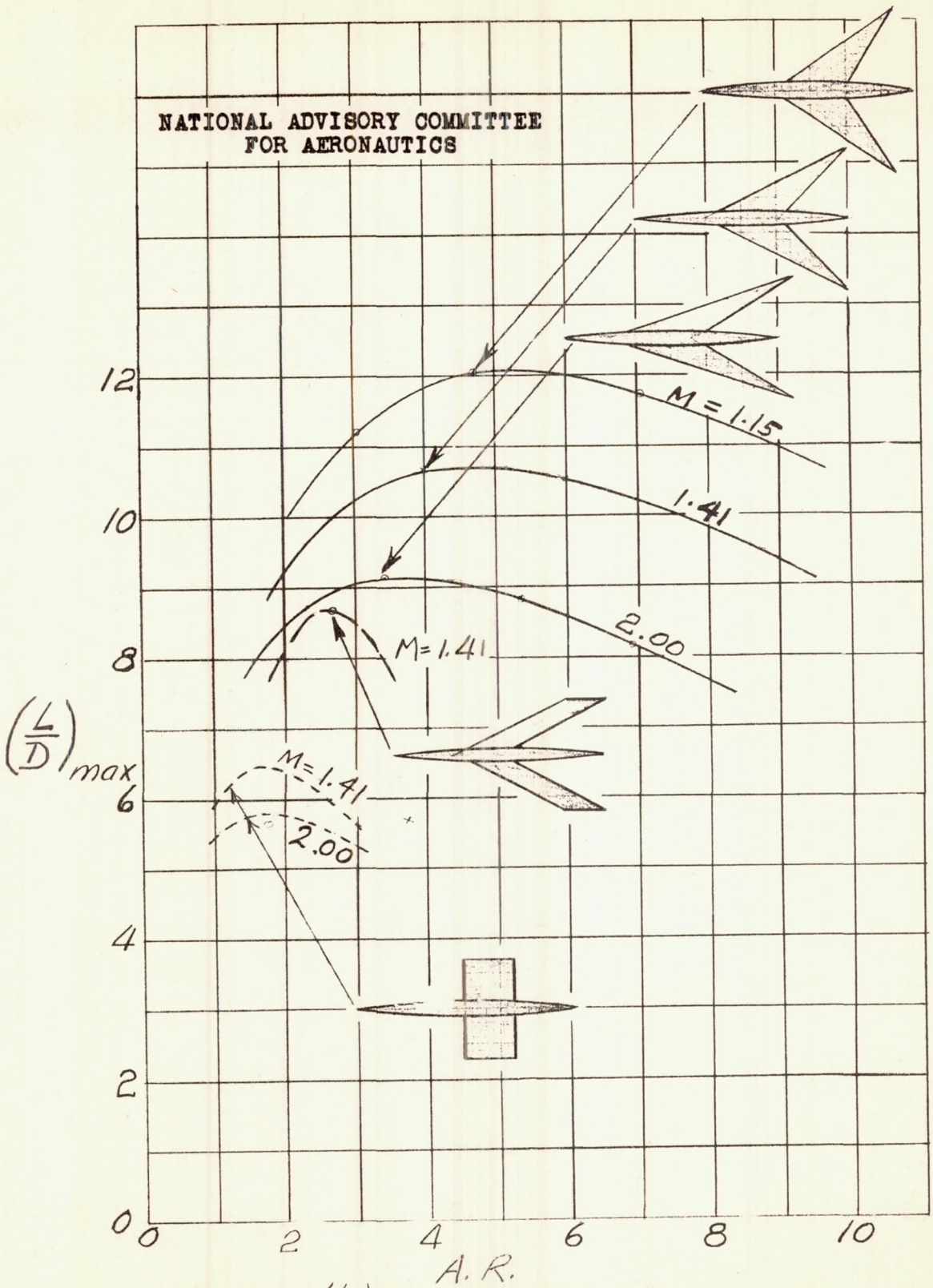


Figure 17.– $\left(\frac{L}{D}\right)_{max}$ at different Mach numbers for airplanes with straight and swept-back wings of varying aspect ratio.